PAPER • OPEN ACCESS

Near-term quantum algorithms for linear systems of equations with regression loss functions

To cite this article: Hsin-Yuan Huang *et al* 2021 *New J. Phys.* **23** 113021

New Journal of Physics
The open access journal at the forefront of physics

Deutsche Physikalische Gesellschaft DPG
IOP Institute of Physics

Published in partnership with: Deutsche Physikalische Gesellschaft and the Institute of Physics

OPEN ACCESS

RECEIVED
18 December 2020

REVISED
20 September 2021

ACCEPTED FOR PUBLICATION
22 October 2021

PUBLISHED
15 November 2021

PAPER

Near-term quantum algorithms for linear systems of equations with regression loss functions

Hsin-Yuan Huang[1,2], **Kishor Bharti**[3] and **Patrick Rebentrost**[3,*]

[1] Institute for Quantum Information and Matter, California Institute of Technology, United States of America
[2] Department of Computing and Mathematical Sciences, California Institute of Technology, United States of America
[3] Centre for Quantum Technologies, National University of Singapore, Singapore
[*] Author to whom any correspondence should be addressed.

E-mail: hsinyuan@caltech.edu, kishor.bharti1@gmail.com and cqtfpr@nus.edu.sg

Keywords: linear systems, quantum computing, near-term quantum algorithms

Abstract

Solving linear systems of equations is essential for many problems in science and technology, including problems in machine learning. Existing quantum algorithms have demonstrated the potential for large speedups, but the required quantum resources are not immediately available on near-term quantum devices. In this work, we study near-term quantum algorithms for linear systems of equations, with a focus on the two-norm and Tikhonov regression settings. We investigate the use of variational algorithms and analyze their optimization landscapes. There exist types of linear systems for which variational algorithms designed to avoid barren plateaus, such as properly-initialized imaginary time evolution and adiabatic-inspired optimization, suffer from a different plateau problem. To circumvent this issue, we design near-term algorithms based on a core idea: the classical combination of variational quantum states (CQS). We exhibit several provable guarantees for these algorithms, supported by the representation of the linear system on a so-called ansatz tree. The CQS approach and the ansatz tree also admit the systematic application of heuristic approaches, including a gradient-based search. We have conducted numerical experiments solving linear systems as large as $2^{300} \times 2^{300}$ by considering cases where we can simulate the quantum algorithm efficiently on a classical computer. Our methods may provide benefits for solving linear systems within the reach of near-term quantum devices.

1. Introduction

Quantum computing promises speedups for problems such as integer factoring and search. Speedups have also been discussed for finding approximate solutions to linear systems of equations and convex optimization [1–6]. Many of these algorithms require a large amount of low-decoherence and fully connected quantum bits, beyond the reach of near-term available quantum computing hardware. As noisy intermediate-scale quantum (NISQ) devices [7] reach sizes of more than 50 qubits, a large amount of research has been devoted to finding tasks where such devices can outperform classical computers. One area of research concerns so-called 'quantum supremacy' [8–13], which is about exhibiting a task for which the classical simulation is conjectured to be hard but which is performed efficiently on a quantum device. While the theoretical guarantees are sound, usually such tasks do not have straightforward practical applications, such as in the case of Boson sampling [14] or random circuits [15]. Many investigations focus on finding applications for near-term quantum computers [16, 17]. Such applications are believed to be in quantum chemistry, optimization and machine learning, and possible algorithmic candidates are the variational quantum eigensolver (VQE) [18–20] and quantum approximate optimization (QAOA) [21, 22].

Due to the constraints of near-term quantum computing devices, such algorithms attempt to minimize the number of qubits and the circuit depth, while still providing a quantum advantage. For the data input, full-scale implementations of conventionally assumed 'oracle' inputs or quantum access memories are not available at the moment. Hence in the near-term often one assumes a data input that is explicitly a set of

low-depth quantum circuits. For the algorithm itself, ancilla-controlled quantum operations can have a substantial gate overhead. To minimize the circuit depth, one aims to keep such operations to a minimum, for example relying only on a single ancilla qubit for the Hadamard test and preferably not even that. Moreover, repetitions of an experiment are often cheap and fast. Hence it can be beneficial to trade the circuit depth for repetitions: instead of preserving coherence till the end of the computation, perform measurements in the intermediate stages and extract useful information. Consider also the final output of the computation. Classically exhibiting the complete solution of the problem can require many repetitions. Hence, we would like to extract a small amount of useful classical information, say the expectation value of some observable. In addition, for near-term quantum computers it might be beneficial to focus on certain types of solutions, i.e. solutions that make a certain loss function small but not others, by saving further computational resources. Hence, near-term quantum computing requires appr s and algorithms that are modifications of, or entirely different from, the algorithms constructed in the more far-term general quantum computational model.

Linear systems are important in a large variety of applications in engineering and science. A common case is when the linear system is specified by a square diagonalizeable matrix $A \in \mathbb{R}^{N\times N}$ and a right-hand side vector $b \in \mathbb{R}^N$. The task is to find a solution vector $x \in \mathbb{R}^N$ for which $Ax = b$ with certain accuracy. Depending on the rank of the matrix and the vector b, the task of solving the linear system takes on various forms. If the matrix is full rank, any vector b can be expressed as a linear combination of the columns of the matrix and matrix inversion finds a unique solution to the linear system. If the matrix has a rank smaller than the dimension, the vector may lie outside the column space of the matrix. In this case, the pseudoinverse of the matrix applied to b finds the smallest ℓ_2 norm approximate solution. Several quantum algorithms related to solving linear system of equations have been proposed, such as HHL [1], Fourier and Chebyshev expansions [23] using linear combination of unitaries (LCU) [24], quantum singular value transformation [25], quantum signal processing and qubitization [26, 27], adiabatic [28] and adiabatic-inspired randomization [29]. A rather unconventional input model is when the matrix is given as a small linear combination of shallow unitaries (LCU). Many physical Hamiltonians have an LCU form, for example a nearest-neighbor spin-chain, and this form is also advantageous for NISQ linear systems solving but does not immediately connect to many practical applications. Other models such as the sparse matrix oracle model can formally, and with considerable overhead, be translated to LCU [30].

In this work, we study near-term quantum algorithms for solving linear systems. We use three loss functions, corresponding to a standard two-norm regression, Tikhonov regression, and a Hamiltonian ground-state encoding, where the respective loss function defines the meaning of 'solving the linear system'. Given the LCU input model for the linear system, we first analyze basic variational algorithms using the Hamiltonian loss function. In variational algorithms, the quantum computer is used to prepare candidates for the solution vector, using a shallow sequence of parameterized quantum gates. Then, measurements are performed on the solution candidate to evaluate the quality of the candidate defined in terms of the loss function. An optimization loop updates the variational parameters to improve the quality of the solution candidate. We propose two types of ansätze for these basic variational algorithms. The first one uses gate sequences that are hardware-efficient, and without explicit usage of the matrix A and b, hence is called the 'agnostic' ansatz. Such agnostic ansätze can be used in various forms of optimization methods, such as the Nelder–Mead method [31], imaginary-time evolution [32, 33], or adiabatic-inspired optimization [34]. The second ansatz, an alternating operator ansatz, is strongly dependent on the linear system and fully uses A and b via Hamiltonian simulation [24, 26, 27, 35, 36]. This approach is inspired by the adiabatic approach and the QAOA method. The drawback is the more far-term nature of the approach. We note other works that investigate the use of variational algorithms to solve linear systems [30, 37], which share similarities with the above ideas.

We encounter simple types of linear systems which exhibit a potential problem for variational approaches. For these linear systems, any pre-specified ansatz with a polynomial number of variational parameters will have a mostly flat optimization landscape with large loss function, which can be considered as a type of plateau effect. A flat optimization landscape will thwart any optimization techniques to find the optimum. We analyze various efforts that circumvent the known barren plateau issue [38], such as properly-initialized imaginary time evolution or the adiabatic-inspired optimization. We show that these attempts may still exhibit the plateau effect, which motivates further efforts and alternative ideas to solve large-scale linear systems with near-term quantum devices and achieve quantum advantage.

To provide a potential solution to the aforementioned problems, we pursue a different route and propose a different class of algorithms for solving linear systems on near-term quantum devices. These algorithms use the two-norm regression and Tikhonov loss functions, hence the obtained solutions may not agree with the Hamiltonian loss function. These algorithms are based on a concept we call classical combination of variational quantum states (abbreviated as CQS). As the name suggests, we show that

different quantum states, variational or not, can be combined via classical pre- and post-processing to increase the power of near-term quantum computers. This combination avoids difficulties in optimizing the variational parameters and provides some provable guarantees for solving linear systems. We introduce the notion of an ansatz tree and show how to find a good set of quantum states and the optimal combination coefficients. We show that at enough depth the ansatz tree is guaranteed to include the solution, and also study the case of Tikhonov regularized regression. We introduce a heuristic approach for judiciously pruning the tree in the less important branches and expanding the tree in the more important branches. Our proposed heuristics is called the gradient expansion heuristics, and can be considered as just one example of many potential heuristics for CQS and the ansatz tree. To demonstrate the potential of this class of algorithms, we have conducted numerical simulations for solving linear systems with sizes up to $2^{300} \times 2^{300}$. Finally, we show that a variation of the CQS method can achieve a similar provable guarantee as existing quantum algorithms for linear systems and can improve upon a recent work [29], reducing the quantum gate count by $(1/\epsilon)$-fold, where ϵ is the desired error to the optimal solution (e.g. $\epsilon = 0.01$), while maintaining the use of only one ancilla qubit. The reduction in quantum gate count comes at the cost of having to run much more measurement repetitions, but we do not need to maintain coherence between the different repetitions. While the overall gate count would increase, the ability to execute a much shorter circuit for each repetition could allow the method to run on a more near-term quantum device.

2. Classical and quantum setting

Before discussing the setting we introduce some notation for this work. Given a matrix A, the spectral norm is denoted by $\|A\|$. The condition number of A is denoted by κ and defined as the ratio of the largest to smallest singular value of A. With A^{-1} the pseudoinverse of A, note the identity $\kappa = \|A\|\|A^{-1}\|$. We also denote the two-norm of a vector by $\|v\|_2 = \sqrt{v^\dagger v}$. We denote with $|0^n\rangle$ an n-qubit register initialized in the all 0 state. The Pauli matrices are denoted by X, Y, and Z. For a quantum state $|b\rangle = \sum_{i=1}^N b_i |i\rangle \in \mathbb{C}^N$ and a classical vector $v \in \mathbb{C}^N$ we naturally use inner products such as $\langle b| v = \sum_{i=1}^N b_i^* v_i$.

We are given a Hermitian matrix $A \in \mathbb{C}^{N\times N}$ with spectral norm $\|A\| \leqslant 1$. Assume without loss of generality that $N = 2^n$. For non-Hermitian matrices, the standard Hermitian embedding can be used. The right-hand side vector $b \in \mathbb{C}^N$, which we assume to be normalized and write in quantum notation as $|b\rangle$. The normalization is not a major restriction as we could rescale the norm of x. The main task is to find a vector x that approximately solves the system of equations. Solving the system here means that given a loss function $L(A, b, x)$, we would like to find x such that

$$L(A, b, x) \leqslant L(A, b, x^*) + \epsilon, \tag{1}$$

where $\epsilon > 0$ and x^* is the minimizer of $L(A, b, \cdot)$. In the quantum setting, we have to make assumptions about the access to the linear system. First, we require quantum access to the right-hand side vector, i.e. a quantum circuit that prepares the vector $|b\rangle$ as a quantum state.

Assumption 1. Assume availability of an efficient n-qubit quantum circuit described by the unitary U_b such that $U_b |0^n\rangle = |b\rangle$.

Next, we require access to the matrix defining the linear system. Here, our main assumption is that the matrix is given by a small linear combination of known unitaries. We note that it is hard in general to find LCUs for arbitrary matrices. In particular, most matrices will not have an efficient LCU decomposition with $\mathcal{O}\left(\text{poly}(\log N)\right)$ terms. Nevertheless, reference [30] shows a formal mapping of sparse oracle access to LCU.

Assumption 2. Assume an efficient unitary decomposition of the matrix $A \in \mathbb{C}^{N\times N}$, i.e. $A = \sum_{k=1}^{K_A} \beta_k U_k$, with $K_A = \mathcal{O}\left(\text{poly}(\log N)\right)$ and unitaries $U_k \in \mathbb{C}^{N\times N}$ with known efficient quantum circuits. We can always absorb the phase of β_k into U_k, so we can assume $\beta_k > 0$. Denote by $B := \sum_{k=1}^{K_A} |\beta_k|$, which we assume to be $B = \mathcal{O}\left(\text{poly}(\log N)\right)$.

Note that $\|A\| \leqslant B$. Next, we discuss the main loss functions used in this work. The first loss function is the well-known ℓ_2-norm loss used in regression methods. This loss function is convex in x.

Definition 1 (Regression loss). Let the linear system be given by $A \in \mathbb{C}^{N\times N}$ and $|b\rangle \in \mathbb{C}^N$. Define the loss function $L_{\text{Reg}}(x) := \|Ax - |b\rangle\|_2^2 = x^\dagger A^\dagger A x - 2\,\text{Re}\{\langle b| Ax\} + 1$.

In other cases, one may want to solve a regularized version of the linear system problem. This version is common in statistics and machine learning, and is known as Tikhonov regularization [39], or ridge

regression [40]. Note that the problem is different from the original linear systems problem and solving it will in general lead to a different solution.

Definition 2 (Tikhonov loss). Let the linear system be given by $A \in \mathbb{C}^{N\times N}$ and $|b\rangle \in \mathbb{C}^N$. Let $\eta = (0, 1]$. Define the loss function $L_{\mathrm{Tik},\eta}(x) := \frac{\eta}{2}\|x\|_2^2 + \|Ax - |b\rangle\|_2^2$. Define $L_{\mathrm{Tik}}(x) := L_{\mathrm{Tik},1}(x)$.

The regularization with $\eta > 0$ turns the loss function into a strongly convex function. To simplify some equations we choose 1 as the upper bound for η. The third loss function is obtained by defining a Hamiltonian which has a unique ground state that is the solution to the linear system. We use techniques presented in [29] for solving the linear system via a method inspired by adiabatic quantum computation. To keep the adiabatic Hamiltonian positive semi-definite across the adiabatic sweep, an ancilla has been introduced in definition 3.

Definition 3. Let $A \in \mathbb{C}^{N\times N}$ be Hermitian and invertible with $\|A\| \leqslant 1$. Define an extended matrix $A(s) := (1-s)Z \otimes \mathbb{1} + sX \otimes A$. In addition, define the parameterized Hamiltonian $H(s) := A(s)P_{+,b}^{\perp}A(s)$, with the projector $P_{+,b}^{\perp} := \mathbb{1} - |+, b\rangle\langle+, b|$.

Among other properties, in [29] it was shown that $H(1)$ has a unique ground state with zero eigenvalue given by $|+\rangle|x^*\rangle = |+\rangle\frac{A^{-1}|b\rangle}{\|A^{-1}|b\rangle\|_2}$, which is proportional to the solution $A^{-1}|b\rangle$ after removing the ancilla. This Hamiltonian implies the following loss function.

Definition 4 (Hamiltonian loss). Define the loss function $L_{\mathrm{Ham}}(|x\rangle) := \langle+, x|H(1)|+, x\rangle$.

The loss function can also be written as $L_{\mathrm{Ham}}(|x\rangle) = \langle x|A^2|x\rangle - \langle x|A|b\rangle\langle b|A|x\rangle$ without the ancilla.

3. Variational algorithms and ansätze

We first discuss basic variational algorithms for solving linear systems. A typical variational algorithm works as follows: one prepares multiple copies of a parameterized quantum state ansatz and measures observables on it; the measurement results provide an estimate of the loss function. An optimization loop changes the parameters of the ansatz with the goal of minimizing the loss function. In this section, we consider two types of variational ansätze. Different ansätze require different assumptions on the available hardware and can lead to different sets of solutions.

- Agnostic ansatz: we take ansätze which perform single qubit rotations and entangling operations. We do not take into account information of the linear system itself except by measuring the loss function.
- Alternating operator ansatz: we alternate the use of operators constructed from A and the vector $|b\rangle$ for generating the ansatz. This requires Hamiltonian simulation of operators derived from A and $|b\rangle\langle b|$.

In particular, we focus on minimizing the Hamiltonian loss function $L_{\mathrm{Ham}}(|x\rangle)$, which is equivalent to finding the ground state of the Hamiltonian $H(1)$. This allows the use of tools such as VQE in quantum chemistry to solve linear systems of equations. The detailed procedure to measure the Hamiltonian loss function is discussed in appendix A.

3.1. Details on variational algorithms for optimizing the ansatz

We first discuss the details of variational algorithms. We consider an ansatz generated by a quantum circuit parametrized by θ, i.e. $|\psi(\theta)\rangle = U_{\mathrm{ansatz}}(\theta)|0^n\rangle$. First, we show the basic VQE for finding the ground state of a Hamiltonian H. Initialize the variational parameters θ to be θ_{init}. While θ has not converged, do the following steps:

(a) Prepare quantum state $|\psi(\theta)\rangle$ on the quantum computer.
(b) Obtain an estimate for the loss function defined by $\langle\psi(\theta)|H|\psi(\theta)\rangle$.
(c) Update θ according to the obtained estimate of the loss function (e.g. using Nelder–Mead).

In addition to using Nelder–Mead, another strategy for optimizing the variational paramete[illegible]rough the use of imaginary tim[illegible]pagation. Imaginary time propagation for Hamiltonian H, initial state $|\psi\rangle$, and time t is defined as [illegible]$\psi\rangle$ with subsequent normalization. With large enough t, the initial state ideally is transformed to the ground state of the Hamiltonian as all excited states will be quickly suppressed. As reference [41] shows, instead of propagating the quantum system, one can directly propagate the parameters θ. The detailed algorithm works as follows. Set $\theta(0) = \theta_{\mathrm{init}}$. For $t = 0, \delta t, 2\delta t, \ldots, T$, do th[illegible] steps:

(a) Obtain an estimate for all terms $C_i(t)$ and $M_{ij}(t)$ using copies of $|\psi(\theta(t))\rangle$, where $M_{ij}(t) = \mathrm{Re}\left\{\left(\frac{\partial}{\partial\theta_i}|\psi(\theta(t))\rangle\right)^\dagger \frac{\partial}{\partial\theta_j}|\psi(\theta(t))\rangle\right\}$ and $C_i(t) = \mathrm{Re}\left\{\left(\frac{\partial}{\partial\theta_i}|\psi(\theta(t))\rangle\right)^\dagger H|\psi(\theta(t))\rangle\right\}$.

(b) Perform variational imaginary time propagation: $\theta(t+\delta t) \leftarrow \theta(t) - M^{-1}(t)C(t)\delta t$.

Each step will obtain a state $|\psi(\theta(t+\delta t))\rangle$ which is approximately the propagated (and renormalized) state $e^{-\delta t H}|\psi(\theta(t))\rangle$. An approach to improve convergence to the solution is based on adiabatic evolution. Adiabatic evolution gradually changes the Hamiltonian $H(s)$ from the initial Hamiltonian (at $s = 0$) to the target Hamiltonian (at $s = 1$). In the VQE setting, an adiabatic-assisted optimization was used in [42, 43]. We follow [43] and refer to this approach as the adiabatic-assisted VQE (AAVQE). To implement AAVQE, we discretize s into T adiabatic steps, $s_0 = 0, s_1, \ldots, s_{T-1}, s_T = 1$. At each adiabatic step t, we use the optimized variational parameter θ^*_{t-1} for $H(s_{t-1})$ as the initial guess for $H(s_t)$. We first initialize θ to be θ^*_0, where $|\psi(\theta^*_0)\rangle$ is the ground state for the initial Hamiltonian $H(0)$. Then, for $t = 1, \ldots, T$, we perform Nelder–Mead or imaginary time propagation on the parameter θ to find an optimized variational parameter θ^*_t for $H(s_t)$ by starting from θ^*_{t-1}.

3.2. Agnostic ansatz

We consider a pre-specified ansatz with several layers, where each layer consists of single-qubit rotations for every qubit and a set of controlled NOT (CNOT) gates for entangling different qubits. The variational parameters are the rotation angles in the single-qubit rotations. This ansatz does not take explicit account of the linear systems A, b and hence we use the name agnostic ansatz. We have performed numerical experiments on the Rigetti quantum virtual machine [44] with system sizes up to $N = 16$ and explored various patterns of how the CNOT gates are applied. We observed that most CNOT gate patterns are able to find the solution as one increases the number of layers and hence also increases the number of variational parameters. We have also tested the AAVQE algorithm [42, 43]. The average accuracy (average fidelity of the output vector with the actual solution over randomly generated linear systems) approaches unity as one increases the number of adiabatic steps. In particular, we observed an improvement using AAVQE over standard VQE. For plots and detailed findings, please refer to appendix F.

3.3. Alternating operator ansatz

We now discuss a different ansatz that contains information about the linear system, i.e. the matrix A and the vector b. This ansatz comes at the cost of requiring Hamiltonian simulation of operators involving A and b. The ansatz is inspired by the method presented in [29] for solving the linear system via adiabatic techniques. In addition, the ansatz is related to reference [45], which considers the alternation of more general families of operators than the original idea of alternating problem Hamiltonian and mixer Hamiltonian [21]. We can write out the Hamiltonian in definition 3 as

$$H(s) = (1-s)^2\mathbb{1} + s^2\mathbb{1}\otimes A^2 - (1-s)^2|-,b\rangle\langle-,b| - s^2(\mathbb{1}\otimes A)|+,b\rangle\langle+,b|(\mathbb{1}\otimes A) - s(1-s)\left(|+,b\rangle\langle-,b|(\mathbb{1}\otimes A) + (\mathbb{1}\otimes A)|-,b\rangle\langle+,b|\right).$$

Examining the Hamiltonian leads to four Hermitian operators that make up $H(s)$, which are scaled by combinations of s and $\pm(1-s)$. The Hamiltonians are $H_1 = A^2$, $H_2 = |-,b\rangle\langle-,b|$, $H_3 = (\mathbb{1}\otimes A)|+,b\rangle\langle+,b|(\mathbb{1}\otimes A)$, and $H_4 = |+,b\rangle\langle-,b|(\mathbb{1}\otimes A) + (\mathbb{1}\otimes A)|-,b\rangle\langle+,b|$, aside from the identity matrix.

Based on the four Hamiltonians H_1, H_2, H_3, and H_4, we can construct an alternating operator ansatz, which is a direct translation of the approach in [29] into the QAOA framework [21]. Let us define the ansatz as follows. Let p be the number of layers of alternating unitaries. For a set of variational parameters $\theta_{k,j}$, $k \in [p]$ and $j \in [4]$, we define the parameterized unitaries corresponding to the four Hamiltonians, $U_j(\theta_{k,j}) := e^{-i\theta_{k,j}H_j}$. Then our variational ansatz is

$$U_4(\theta_{p,4})U_3(\theta_{p,3})U_2(\theta_{p,2})U_1(\theta_{p,1})\ldots U_4(\theta_{1,4})U_3(\theta_{1,3})U_2(\theta_{1,2})U_1(\theta_{1,1})|b\rangle.$$

This ansatz contains explicit information of A and b, which avoids potential problems in variational algorithms discussed in section 3.4. However, the suitability of this method for the use in near-term quantum computers depends on the difficulty of simulating the unitaries $U_j(\theta_{k,j})$. Given assumptions 1 and 2, we can express the Hamiltonians as $H_1 = \sum_{k,k'=1}^{K_A}\alpha_k\alpha_{k'}U_{k'}U_k$, $H_2 = (\mathbb{1}\otimes U_b)|-,0^n\rangle\langle-,0^n|(\mathbb{1}\otimes U_b^\dagger)$, $H_3 = \sum_{k,k'=1}^{K_A}\alpha_k\alpha_{k'}U_k(\mathbb{1}\otimes U_b)|+,0^n\rangle\langle+,0^n|(\mathbb{1}\otimes U_b^\dagger)U_{k'}$, and $H_4 = \sum_{k=1}^{K_A}\alpha_k(\mathbb{1}\otimes U_b)|+,0^n\rangle\langle-,0^n|(\mathbb{1}\otimes U_b^\dagger)(\mathbb{1}\otimes U_k) + (\mathbb{1}\otimes U_k)(\mathbb{1}\otimes U_b)|-,0^n\rangle\langle+,0^n|(\mathbb{1}\otimes U_b^\dagger)$. As these operators are combinations of unitaries and projectors, Hamiltonian simulation for simple cases may be within the realm of near-term

hardware. However, at this point, there are no guarantees on performance due to the potentially difficult optimization of the variational parameters $\theta_{k,j}$.

3.4. Potential problems in variational algorithms for solving linear systems

Typical optimization for linear systems minimizing $\|Ax - |b\rangle\|_2^2$ from definition 1 is convex in x. The gradient is larger when we are further away from the optimal solution and the negative gradient always points in the descent direction. On the other hand, when we restrict to the variational quantum state space, the optimization landscape is no longer convex and not well understood in many cases. We consider classes of linear systems that show difficulties when using variational methods. The difficulties arise essentially from the fact that a random linear system in an exponentially large Hilbert space will have solutions that only have exponentially small overlap with the ansatz $|\psi(\theta)\rangle$ under most parameters θ. The setting is reminiscent of Grover search/amplitude amplification: starting from an initial state (such as the uniform superposition), the goal is to amplify some part of the Hilbert space (such as a single computational basis state). The Grover lower bound states that this amplification in general cannot be done faster than $\sqrt{2^n}$, where n is the number of qubits. We exhibit a plateau effect associated with this well-known lower bound for a class of linear systems. The class of linear systems may be called 'randomized needle-in-a-haystack' linear systems, since they have a single random bit-string and associated computational basis state as their defining characteristic. While this plateau may extend to a broader class of linear systems than discussed here, we note that it does not preclude the existence of certain classes of linear systems and ansätze in combination with properly chosen loss functions for which variational optimization can provide quantum advantages. Linear systems with additional structure may be one example and a better characterization of such linear systems is left for future work. In section 4, we provide a method to potentially overcome the issues discussed here.

The following proposition gives for a class of linear systems a general bound on the gradient of the loss functions using an arbitrary variational quantum state. After the proposition, we argue that this gradient bound is exponentially small for many ansatz states.

Proposition 1 (Gradient bound for random linear systems). *Consider a class of linear systems where $|b\rangle = |0^n\rangle$ and A is a tensor product of Pauli-X matrices and an arbitrary ansatz $|x(\theta)\rangle$, $\theta \in \mathbb{R}^m$. There exists a probability distribution over A, such that for any initial point θ^0, we have*

$$\left|\frac{\partial}{\partial\theta_i}\|A\,|x(\theta)\rangle - |b\rangle\|_2^2\Big|_{\theta=\theta^0}\right| \leqslant \frac{2}{2^{n/4}}\left\|\frac{\partial}{\partial\theta_i}\,|x(\theta)\rangle\Big|_{\theta=\theta^0}\right\|, \quad \forall\, i = 1,\ldots,m, \tag{2}$$

with probability at least $1 - m/2^{n/2}$. Similarly, we have

$$\left|\frac{\partial}{\partial\theta_i}\,\langle x(\theta)|\,(A^2 - A\,|b\rangle\,\langle b|\,A)\,|x(\theta)\rangle\Big|_{\theta=\theta^0}\right| \leqslant \frac{2}{2^{n/4}}\left\|\frac{\partial}{\partial\theta_i}\,|x(\theta)\rangle\Big|_{\theta=\theta^0}\right\|, \quad \forall\, i = 1,\ldots,m, \tag{3}$$

with probability at least $1 - m/2^{n/2}$.

The proof is given in appendix B. For many ansätze, we have $\left\|\frac{\partial}{\partial\theta_i}\,|x(\theta)\rangle\right\| = \mathcal{O}(1)$, which implies the bound $2/2^{n/4}$. For example, consider an ansatz where the variational parameters parameterize Pauli rotations,

$$|x(\theta)\rangle = V(\theta_{\neq i})\exp(\mathrm{i}P\theta_i)\,U(\theta_{\neq i})\,|0^n\rangle\,, \tag{4}$$

where P is a tensor product of Pauli operators, $\theta_{\neq i}$ contains all parameter except for the ith variational parameter. Then we have

$$\left\|\frac{\partial}{\partial\theta_i}\,|x(\theta)\rangle\right\| = \|V(\theta_{\neq i})\mathrm{i}P\,\exp(\mathrm{i}P\theta_i)\,U(\theta_{\neq i})\,|0^n\rangle\| = 1. \tag{5}$$

In cases such as these, when $\left\|\frac{\partial}{\partial\theta_i}\,|x(\theta)\rangle\right\| \leqslant 1$, the proposition shows that for both loss functions definition 1 (the regression loss function) and definition 4 (the Hamiltonian loss function), the loss function will be flat at that point with an exponentially small slope with high probability, an effect that can be referred to as a barren plateau. In this case, the plateau effect appears for all initial variational parameters, whenever the number of parameters m is much smaller than $2^{n/2}$, and independent of the specific structure of the variational ansatz. The behavior appears even for shallow circuits. A numerical experiment that demonstrates this behavior can be seen in figure 1. From the figure, we can clearly see the appearance of the plateau as the system size grows larger.

Whenever the loss function landscape is essentially flat, the presence of small errors due to statistical fluctuations in the quantum measurements would make it very hard for existing optimization approaches to

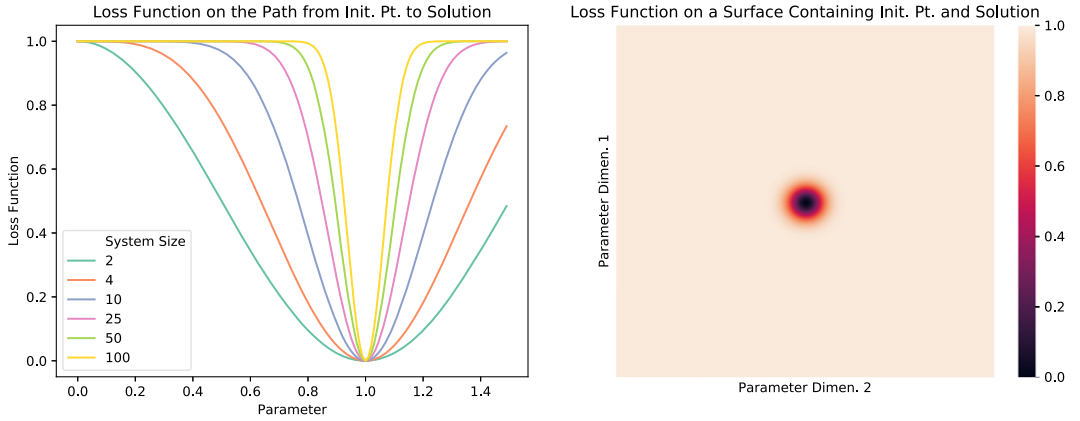

Figure 1. The optimization landscape of variational linear system solver for a random matrix $A = (\sigma_x^{(1)})^{k_1} \otimes \cdots \otimes (\sigma_x^{(n)})^{k_n}$ with $k \in \{0,1\}^n$, $\|k\|_0 = \lceil n/2 \rceil$, and $|b\rangle = |0^n\rangle$. We consider the variational ansatz given by $|x(\theta)\rangle = e^{-i\theta_1 \sigma_x^{(1)}} \otimes \cdots \otimes e^{-i\theta_n \sigma_x^{(n)}} |0^n\rangle$. Left: here, we plot a one-dimensional cut through the high-dimensional landscape, tracing along a line connecting the initial point (parameter $= 0$) and the optimal solution (parameter $= 1$) for varying system size. We can clearly see the appearance of a plateau with the solution being a sharp valley at some point in the high-dimensional surface. Right: we plot the landscape on a surface that contains the initial point (bottom left corner with loss function $= 1.0$) and the optimal solution (the middle point with loss function $= 0.0$) for a system with $n = 100$. The loss function is near flat everywhere except a sharp hole in the middle that contains the solution.

find the optimal solution efficiently even if there exists a solution in the ansatz. For example, if we use variational imaginary time evolution as described in section 3.1 to optimize the variational parameters, the same analysis shows that $C(t)$ used in the propagation of θ would be an exponentially small vector. This means even if $C(t)$ is measured to exponential precision (which already requires exponential time due to the statistical error from the quantum measurements), the imaginary time propagation would still take exponential time to find the ground state.

The conclusion is that for variational algorithms with a pre-specified ansatz, such as the agnostic ansatz or a hardware efficient ansatz, it could be challenging to solve many linear systems due to the flat landscape of the loss functions. One important note is that our plateau effect originates from a different cause compared to the barren plateau problem [38], which appears in an ansatz initialized as a random quantum circuit with enough depth. This is not to say that variational quantum algorithms are hopeless in achieving quantum advantages for linear systems. If we have a way of finding an ansatz with an initial parameter that is close to the solution by making use of structure in A, $|b\rangle$, then this problem could be circumvented. For example, an ansatz that contains explicit application of A, such as e^{-iAt}, in its variational circuit does not fall into this problem. The alternating operator ansatz proposed in section 3.3 is such a choice that may be able to avoid this problem, but requires further study of convergence guarantees and the optimization of variational parameters may also be hard. In the next section, we aim to propose an alternative approach that potentially circumvents the problem discussed here and offers the ability to derive some provable guarantees.

4. Classical combination of quantum states for linear systems

4.1. Main idea

Most hybrid quantum–classical algorithms parameterize the quantum state with classical parameters, and have the quantum state created on the quantum processor. To extend the reach of near-term quantum devices, we consider a different way to generate manipulable states. Let the $N = 2^n$-dimensional Hilbert space be $\mathcal{H}$. Let $W(\theta)$ denote an n-qubit circuit with k real parameters $\theta \in \mathbb{R}^k$. Also let $\mathcal{V}_W = \{|\psi_W(\theta)\rangle = W(\theta)|0^n\rangle \mid \theta \in \mathbb{R}^k\} \subset \mathcal{H}$ denote the corresponding quantum states. A typical variational algorithm is based on a such a parameterized ansatz $\mathcal{V}_W$ and tries to find the best $|\psi_W(\theta)\rangle$ in $\mathcal{V}_W$ by tuning θ. However, there are two drawbacks when using typical variational algorithms.

- $\mathcal{V}_W$ may not be large enough to contain the solution. Such a drawback may often be the case in hardware-efficient ansätze and even the alternating operator ansatz discussed above.
- Even when $\mathcal{V}_W$ contains the solution, the variational parameter θ could be difficult to optimize. This problem can already be seen in the toy examples presented in previous sections.

Given these drawbacks, it is reasonable to develop methods that are fundamentally different from the variational approaches. Here, we investigate a method called classical combination of (variational) quantum

states (CQS). In this classical combination of quantum states, we consider a hybrid quantum–classical state constructed by a set of unitaries. For the general discussion here, we consider parameterized unitaries, similar to the variational approaches. Our extension in that sense contains the previous variational approaches (with the aforementioned problems). In the remainder of this work after this general discussion, we however take the unitaries to be non-parameterized and show only the combination of non-parameterized quantum states.

Let $W_i(\theta_i)$ for $i = 1, \ldots, m$ be quantum circuits with k_i parameters each, $\theta_i \in \mathbb{R}^{k_i}$. We construct a state vector $x \in \mathcal{H}$ as a quantum–classical hybrid,

$$x = \sum_{i=1}^{m} \alpha_i \left|\psi_{W_i}(\theta_i)\right\rangle, \quad \text{where } \alpha_1, \ldots, \alpha_m \in \mathbb{C},\ \theta_1 \in \mathbb{R}^{k_1}, \ldots, \theta_m \in \mathbb{R}^{k_m},$$

where α_i are the combination parameters and θ_i are the usual variational parameters. Both sets of parameters are stored on the classical processor. The state vector $x \in \mathcal{H}$ is never created on the quantum processor. Furthermore x may not be normalized, so it is not a quantum state in general.

To manipulate x with near-term quantum algorithms, the most important aspect is the ability to measure its expectation value for an observable O. We can obtain the expectation value $x^\dagger O x$ by performing quantum measurements and classical post-processing, via the following steps.

(a) Estimate $\left\langle\psi_{W_i}(\theta_i)\right| O \left|\psi_{W_j}(\theta_j)\right\rangle$ using a modified Hadamard test (see proposition 11 in appendix A) on the quantum processor. The modified Hadamard test comes at the cost of preparing $\left|\psi_{W_i}(\theta_i)\right\rangle$ and $\left|\psi_{W_j}(\theta_j)\right\rangle$ in superposition using one additional ancilla.

(b) Compute an estimate of $\sum_{i=1}^{m}\sum_{j=1}^{m}\alpha_i^*\alpha_j \left\langle\psi_{W_i}(\theta_i)\right| O \left|\psi_{W_j}(\theta_j)\right\rangle$ on the classical processor using the estimates from the previous step.

For comparison, suppose for the moment that x is a (normalized) quantum state. To create x on the quantum processor, we need $\mathcal{O}\left(\log(m)\right)$ ancilla qubits and $\mathcal{O}(m)$ controlled unitaries that prepare all $\left|\psi_{W_i}(\theta_i)\right\rangle,\ \forall\ i$ in superposition. We can summarize the improvement in terms of resources using the hybrid quantum–classical state x instead of the corresponding quantum state in the following table. We only show the m dependency and omit any other factors.

Resource	Full quantum state	CQS
Gate count	$\mathcal{O}(m)$	$\mathcal{O}(1)$
Ancilla count	$\mathcal{O}\left(\log(m)\right)$	1
Measurements	$\mathcal{O}(1)$	$\mathcal{O}\left(m^2\right)$

The gate count is that of a single quantum computation using the superposition compared to the classical combination. The gate count in a single quantum run is reduced $\mathcal{O}(m)$-fold. The CQS method comes at the cost of increased number of repetitions, i.e. an increased number of quantum measurements. Here again we only denote the m dependency.

Note that we do not need to maintain quantum coherence between measurements. Hence CQS can be the preferred method on NISQ devices. On such devices, the gate count is often limited due to the errors present in the device, and the space of possible variational quantum states $\mathcal{V}_W$ that can be prepared without error is limited by the gate count. The classical combination of quantum states can provide a considerable improvement upon the space of manipulable states on near-term quantum processors. An illustration of this idea is shown in figure 2.

We now present the *meta*-strategy for finding an $x \in \mathcal{H}$ that solves the linear system of equations. The approach consists of an optimization and an expansion step. The approach may avoid the optimization of θ_i which can involve a complicated optimization landscape. We start with $m = 1$ and a quantum state $\left|\psi_{W_1}(\theta_1)\right\rangle$. Each iteration proceeds as follows.

(a) Optimization: solve for the optimal $\alpha_1^*, \ldots, \alpha_m^* \in \mathbb{C}$ with $x(\alpha) = \sum_{i=1}^{m}\alpha_i \left|\psi_{W_i}(\theta_i)\right\rangle$.

(b) Expansion: using the current optimum $x(\alpha^*) = \sum_{i=1}^{m}\alpha_i^* \left|\psi(\theta_i)\right\rangle$, find a next circuit W_{m+1} with k_{m+1} parameters and a setting $\theta_{m+1} \in \mathbb{R}^{k_{m+1}}$ for those parameters. This circuit generates the state $\left|\psi_{W_{m+1}}(\theta_{m+1})\right\rangle$.

(c) Set $m \leftarrow m + 1$.

A few comments are in order. The step (a) only involves the parameters $\alpha_1, \ldots, \alpha_m \in \mathbb{C}$ and is a convex optimization. This step is described in the next section 4.2. The expansion step (b) assumes that we can find a new circuit W_{m+1}. This circuit may or may not be parameterized by a parameter vector $\theta_{m+1} \in \mathbb{R}^{k_{m+1}}$, the

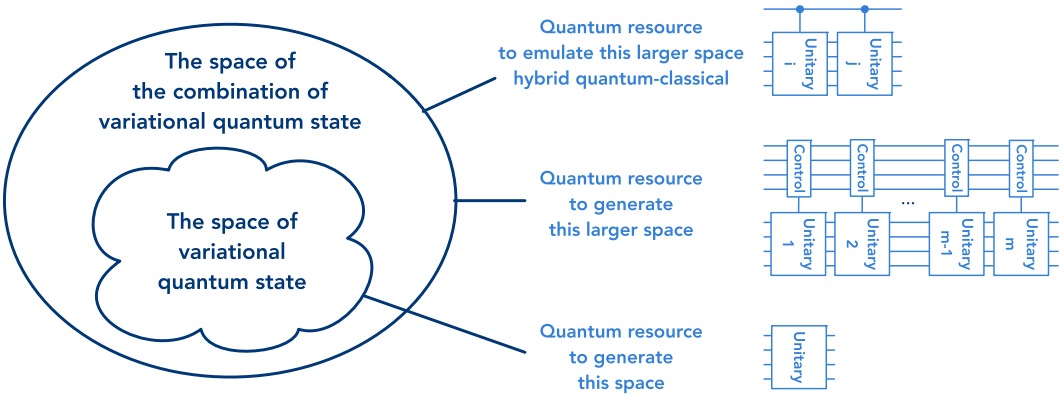

Figure 2. Illustration of our CQS approach. By considering subspaces spanned by m variational quantum states, we are able to represent a larger class of states in the Hilbert space $\mathcal{H}$. The basic concept is illustrated on the left-hand side. In order to generate states in the m-dimensional subspace, we have to increase the quantum resources m-fold (m times more gates and $O(\log(m))$ ancilla qubits that jointly control the unitaries). This case is illustrated by the middle picture on the right-hand side. Using a hybrid quantum–classical emulation, we can operate in this larger space using only a single additional ancilla qubit and twice as many gates, as illustrated in the top picture on the right-hand side.

strategy applies to both cases. Also note that the number of parameters k_{m+1} may not have any particular relationship with the number of parameters of the previous steps $k_1, \ldots, k_m$. In the case that the circuits are indeed parameterized, setting the parameters to useful values may involve optimization, which again may run into the plateau issues discussed in section 3.4.

However, the strategy can also be used without taking into account or optimizing the parameters θ_{m+1} as long as the new state $|\psi_{W_{m+1}}\rangle$ is sufficiently different from the previous states. Indeed, the remainder of this work including the ansatz tree approach in section 4.3 does not explicitly include these parameters.

4.2. Optimization of combination parameters

We first focus on the case when we have selected a good set of $|\psi_{W_1}\rangle, \ldots, |\psi_{W_m}\rangle$, e.g. $A^{-1}|b\rangle \in \text{span}\{|\psi_{W_1}\rangle, \ldots, |\psi_{W_m}\rangle\}$, and we want to optimize over $\alpha_1, \ldots, \alpha_m \in \mathbb{C}$. We will show that the optimization of $\alpha_1, \ldots, \alpha_m$ will always find the optimal solution. To simplify the notation, we let $|u_i\rangle := |\psi_{W_i}\rangle$ from here on. We first define an auxiliary linear system.

Definition 5 (Auxiliary system). Given $A = \sum_{k=1}^{K_A} \beta_k U_k$ via assumption 2 and $|b\rangle$ via assumption 1. For all $i \in [m]$, assume a unitary W_i with $|u_i\rangle := W_i|0^n\rangle$. Define the auxiliary quantities:

(a) The matrix $V := (v_1, \ldots, v_m) \in \mathbb{C}^{2^n \times m}$ with column vectors $v_i := A|u_i\rangle$ and the kernel matrix $(V^\dagger V)_{ij} \equiv \langle u_i| A^\dagger A |u_j\rangle$ for $i, j \in [m]$.

(b) Real and imaginary parts of the kernel matrix as $R := \text{Re}\{V^\dagger V\}$ and $I := \text{Im}\{V^\dagger V\}$, for which $R^T = R$ and $I^T = -I$.

(c) The right-hand side vector $q \in \mathbb{C}^m$ with $q_i := \langle i| V^\dagger |b\rangle = \langle u_i| A^\dagger |b\rangle$ for $i \in [m]$.

(d) Auxiliary system

$$Q := \begin{pmatrix} R & -I \\ I & R \end{pmatrix}, \qquad r := [\text{Re}\{q\}, \text{Im}\{q\}]^T.$$

The reasoning for these definitions will be clarified now. Recall the standard regression loss function

$$L_{\text{Reg}}(x) = \|Ax - |b\rangle\|_2^2 = x^\dagger A^\dagger A x - 2\,\text{Re}\{\langle b| Ax\} + 1,$$

as in definition 1. Given $x = \sum_{i=1}^m \alpha_i |u_i\rangle$, we can reduce the optimization in an exponentially large space $x \in \mathcal{H}$ to an optimization over m variables. Using V, we can simply express the left-hand side of the linear system as $Ax = \sum_{i=1}^m \alpha_i A|u_i\rangle = V\alpha$. Thus, we would like to minimize

$$\|V\alpha - |b\rangle\|_2^2 = \alpha^\dagger V^\dagger V \alpha - 2\,\text{Re}\{q^\dagger \alpha\} + 1,$$

where we are using the vector q. We obtain a regression problem for the combination parameters α with the kernel matrix $V^\dagger V$. We can cast this quadratic optimization problem with complex variables α to a real optimization problem. With the two matrices R and I, for which $R^T = R$ and $I^T = -I$, it is straightforward to see that $\alpha^\dagger V^\dagger V \alpha = \text{Re}\{\alpha\}^T R\,\text{Re}\{\alpha\} + \text{Im}\{\alpha\}^T R\,\text{Im}\{\alpha\} + 2\,\text{Im}\{\alpha\}^T I\,\text{Re}\{\alpha\}$. The recast optimization problem is

$$\min_{z \in \mathbb{R}^{2m}} z^T Q z - 2 r^T z + 1,$$

with the system Q, r. We obtain the α coefficients from the optimization variables by $z = [\mathrm{Re}\{\alpha\}, \mathrm{Im}\{\alpha\}]$.

Once the input quantities Q and r are determined, such a regression problem can be solved via the pseudoinverse. The inputs Q and r can be measured on a quantum computer using the strategies in appendices A and D. However, such measurements result in erroneous estimates of the quantities. The error will translate into an error in the loss function and the proposed solution for the combination parameters α. Using standard results in random matrix theory, we are able to achieve a rigorous bound on the error of the obtained solution, see proposition 2. Appendix D contains the detailed analysis, which is a combination of lemma 2 (measuring Q and r) and proposition 12 (solving the optimization problem).

Proposition 2 (Guarantee for fixed subspace). *Given $A = \sum_{k=1}^{K_A} \beta_k U_k$ via assumption 2 and $|b\rangle$ via assumption 1. For all $i \in [m]$, assume a unitary W_i with $|u_i\rangle := W_i |0^n\rangle$. This defines the auxilliary system Q, r with $z^* := Q^{-1} r$. We can find an $\hat{\alpha} \in \mathbb{C}^m$ such that it is ϵ-close to optimal,*

$$L_{\mathrm{Reg}}\left(\sum_{i=1}^{m} \hat{\alpha}_i |u_i\rangle\right) \leqslant \min_{\alpha_1,\ldots,\alpha_m \in \mathbb{R}} L_{\mathrm{Reg}}\left(\sum_{i=1}^{m} \alpha_i u_i\right) + \epsilon,$$

using $\mathcal{O}\left(m^3 B^4 K_A^2 \|Q\| \left\|Q^{-1}\right\|^2 (1 + \|z^*\|)^2/\epsilon\right)$ quantum measurements.

Proof. We estimate each entry in Q, r independently via lemma 2. To obtain one sample of an entry of Q, r, we need $\mathcal{O}\left(K_A^2\right)$ quantum measurements. Because each sample of an entry results in a value bounded by $\mathcal{O}\left(B^2\right)$, the average of $\mathcal{O}\left(B^4 T\right)$ samples, or $\mathcal{O}\left(B^4 T K_A^2\right)$ quantum measurements, on a single entry gives a random variable with variance $\mathcal{O}\left(1/T\right)$. By performing $\mathcal{O}\left(m^2 \times B^4 K_A^2 T\right)$ quantum measurements, we obtain an independent estimate for all the entries in Q, r. Standard results in random matrix theory [46] (corollary 3.12) give $\left\|\hat{Q} - Q\right\| \leqslant \mathcal{O}\left(\sqrt{m/T}\right)$ and $\|\hat{r} - r\| \leqslant \mathcal{O}\left(\sqrt{m/T}\right)$ with high probability.

From proposition 12, we obtain $T > Cm \|Q\| \left\|Q^{-1}\right\|^2 (1 + \|z^*\|)^2/\epsilon$. The total number of quantum measurements is hence

$$\mathcal{O}\left(m^2 B^4 K_A^2 T\right) = \mathcal{O}\left(m^3 B^4 K_A^2 \|Q\| \left\|Q^{-1}\right\|^2 (1 + \|z^*\|)^2/\epsilon\right).$$

□

We obtain a rather complicated dependency on $\|Q\|$, $\left\|Q^{-1}\right\|$, and $\|z^*\|$. In practice, upper bounds for these quantities could be obtained via further classical pre- and post-processing. For example, given a matrix Q, we can always diagonalize it in time $\mathcal{O}\left(m^3\right)$ and find a well-conditioned approximation Q_ϵ with smallest eigenvalue ϵ. Then compute $z_\epsilon^* := Q_\epsilon^{-1} r$ as the solution to the problem.

Furthermore, we give informal bounds on these quantities. We note that $\|Q\| \leqslant \kappa^2 m$, due to its definition via V and A. The quantity $\left\|Q^{-1}\right\|$ is harder to bound. In principle, the choice of basis could be such that $\left\|Q^{-1}\right\|$ is unbounded in the case when the smallest non-zero eigenvalue of Q is very close to zero. In this case, use the well-conditioned approximation Q_ϵ in the proposition, with the same ϵ as in the proposition. For this matrix one has $\left\|Q_\epsilon^{-1}\right\| \leqslant 1/\epsilon$, which increases the ϵ dependency in the proposition. Finally, note that $\|z_\epsilon^*\| \leqslant \left\|Q_\epsilon^{-1}\right\| \|r\| \leqslant \sqrt{2m}/\epsilon$, using $\|r\| \leqslant \sqrt{2m}$. Employing all these steps, we can express the number of measurements in the proposition as

$$\mathcal{O}\left(m^5 B^4 K_A^2 \kappa^2/\epsilon^5\right). \tag{6}$$

A natural question is whether the problem of solving linear systems will become much easier when we consider optimization over a small subspace $\mathrm{span}(|u_1\rangle, |u_2\rangle, \ldots, |u_m\rangle)$. We can show that finding near-optimal combination parameters in a subspace should be hard for classical algorithms, as it is not believed that BQP = BPP.

Proposition 3 (Informal). *If there is a classical algorithm that efficiently finds the combination parameters of $|u_1\rangle, |u_2\rangle, \ldots, |u_m\rangle$ to minimize $L_{\mathrm{Reg}}\left(\sum_{i=1}^{m} \alpha_i |u_i\rangle\right)$, then BQP = BPP.*

See proposition 13 in appendix D for the complete statement and proof.

4.3. Ansatz tree approach for finding the subspace

We have shown good theoretical properties in the case where the subspace is fixed, i.e. a guarantee for finding a near-optimal solution in the subspace. However, the results so far rely on already knowing a subspace that approximately contains the solution x. Here, we propose an approach that is inspired by the Krylov subspace method for solving linear systems. A Krylov subspace is a subspace spanned by $\{b, Ab, A^2 b, \ldots, A^{r-1} b\}$. The Krylov subspace method solves for the optimal solution in the subspace and increases r if the obtained solution is not good enough.

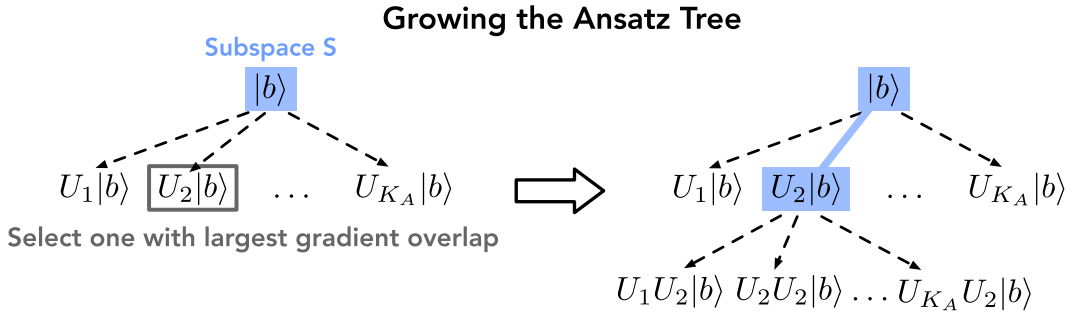

Figure 3. Illustration of the ansatz tree and the gradient expansion strategy. The green region is the current subspace. On the left-hand side, we select a node that is a child of the nodes in the green region and that has the largest overlap with the gradient, here $U_2|b\rangle$. The right-hand side shows the tree after adding the new element to the subspace.

Our approach constructs the subspace by exploring the space of solutions on a tree structure we call the ansatz *tree*. We use the structure of A in assumption 2, in particular the unitaries that make up A, to construct such a tree. The core idea is to associate the nodes of this tree with the subspace states $|u_i\rangle$ from the previous section. We show that a near-optimal solution is guaranteed to be found after enough nodes are included in the ansatz tree. While the size of the tree may be very large in the worst case, the tree allows the systematic use of heuristic approaches to explore, prune, and expand it.

The construction of the full ansatz tree is given in definition 6. We start with the quantum state $|b\rangle$ and recursively construct the child nodes generated by the matrix A. An illustration is shown in figure 3.

Definition 6 (Ansatz tree). Given $|b\rangle$ as in assumption 1 and $A = \sum_{k=1}^{K_A} \beta_k U_k$ as in assumption 2, we define the ansatz tree recursively, as follows.

$$\begin{cases} \text{The root of the tree is } |b\rangle . \\ \text{Each node } |\psi\rangle \text{ on the tree has } K_A \text{ child nodes: } U_1|\psi\rangle, \ldots, U_{K_A}|\psi\rangle . \end{cases}$$

Most straightforwardly one can take all the nodes of the ansatz tree up to some depth as the solution subspace. We now derive guarantees for this approach. These guarantees show that the number of required nodes may be very large. We then discuss a heuristic approach to prune the tree in the less important directions and expand the tree in the more important directions, a method we call *gradient expansion heuristics*. This heuristic can reduce the number of nodes included in the subspace for a good solution.

Taking the full ansatz tree and the regression loss from definition 1, we are guaranteed to find a near-optimal solution after enough depth, see the next proposition.

Proposition 4 (Complete ansatz tree for regression loss function). *Fix $\epsilon > 0$. Given the ansatz tree for A as in definition 6 with $\|A\| = 1$ and $\left\|A^{-1}\right\| = \kappa$, by selecting all nodes $\{|u_1\rangle, \ldots, |u_m\rangle\}$ on the ansatz tree with depth at most $\mathcal{O}\left(\kappa \log \kappa + \kappa \log(1/\epsilon)\right)$, we have*

$$\min_{\alpha_1,\ldots,\alpha_m \in \mathbb{R}} L_{\text{Reg}}\left(\sum_{i=1}^{m} \alpha_i |u_i\rangle\right) \leqslant \min_{x \in \mathbb{C}^{2^n}} L_{\text{Reg}}(x) + \epsilon = \epsilon.$$

The result is an extension and variation of known results on using the polynomial approximation of $1/x$ to solve linear systems of equations [47]. See appendix E for a detailed proof.

The following theorem summarizes this approach in terms of a guarantee for the closeness of obtained solution versus ideal solution. When κ is large, the required depth can be large in the worst case. Proposition 4 implies a large number of nodes on the ansatz tree for a good approximation to the solution. In particular, the number of nodes scales exponentially in the tree depth and thereby in the condition number, i.e. $m = K_A^{\mathcal{O}(\kappa \log(\kappa/\epsilon))}$.

Theorem 1 (Guarantee for solution to regression problem). *Let $|b\rangle$ and A be given as in assumptions 1 and 2. A solution x can be found such that the distance to the respective optimal solution $x^* := \arg\min_{x \in \mathbb{C}^{2^n}} L_{\text{Reg}}(x)$ is*

$$\|x - x^*\|_2^2 \leqslant \epsilon, \tag{7}$$

with high probability using a per-measurement quantum circuit depth

$$\mathcal{O}\left(\kappa \log \kappa + \kappa \log(1/\epsilon)\right) \tag{8}$$

and a basis set size of

$$m = K_A^{\mathcal{O}(\kappa \log(\kappa/\epsilon))}. \tag{9}$$

Proof. The size of the basis set is determined by K_A exponentiated by the tree depth. For finding the optimal α we require the number of measurements quoted in proposition 2, where m is the size of the basis set.

Proposition 4 can be converted to a bound on the distance to the optimal solution. Let $x = \sum_{i=1}^{m} \alpha_i |u_i\rangle$ for the optimal α_i minimizing $L_{\text{Reg}}\left(\sum_{i=1}^{m} \alpha_i |u_i\rangle\right)$. Using proposition 4, we have

$$\epsilon \geqslant L_{\text{Reg}}(x) = (x - A^{-1}b)^{\dagger} A^{\dagger} A (x - A^{-1}b) \geqslant \frac{1}{\kappa^2} \left\| x - A^{-1}b \right\|_2^2. \tag{10}$$

To achieve an ϵ-error in distance to the optimal solution $\left\| x - A^{-1}b \right\|_2^2$, we need to achieve an ϵ/κ^2 error in the loss function. The scaling of tree depth for obtaining a solution close to $A^{-1}b$ is $\mathcal{O}\left(\kappa \log \kappa + \kappa \log(\kappa^2/\epsilon)\right) = \mathcal{O}\left(\kappa \log \kappa + \kappa \log(1/\epsilon)\right)$. □

It is hence important to find special cases and methods to reduce the number of nodes.

4.4. Linear systems with Tikhonov regularization

Next, consider a *regularized* linear system of equations. The problem is specified by the loss function from definition 2. We note that the regularization term is scaled by a parameter η. For $\eta > 0$, it is different to solving the original linear system with the loss function from definition 1 and the solutions can be far from each other. This parameter can be used to find solutions also for L_{Reg}, however the worst case observed in theorem 1 still applies. The next proposition shows the general dependency on η for the Tikhonov regularized problem. The number of nodes is exponential in $1/\eta$, which embodies the worst-case behavior. In addition, it shows that for $\eta = 1$ a polynomial number of nodes is enough to guarantee the performance of the solution even in the worst case. In this case, the depth only depends on how good the approximation is, which is characterized by ϵ.

Proposition 5 (Complete ansatz tree for Tikhonov loss function). *Fix $\epsilon > 0$. Given the ansatz tree for a Hermitian A as in definition 6 with $\|A\| \leqslant 1$, select all nodes $\{|u_1\rangle, \ldots, |u_m\rangle\}$ on the ansatz tree with depth at most d_{Tik}.*

(a) For $\eta \in (0, 1]$, if $d_{\text{Tik}} = \mathcal{O}\left(\frac{1}{\eta} \log(1/\epsilon)\right)$, we have

$$\min_{\alpha_1,\ldots,\alpha_m \in \mathbb{R}} L_{\text{Tik},\eta}\left(\sum_i \alpha_i |u_i\rangle\right) \leqslant \min_{x \in \mathbb{C}^{2^n}} L_{\text{Tik},\eta}(x) + \epsilon.$$

(b) If $d_{\text{Tik}} \geqslant \lceil C \log(1/2\epsilon) \rceil$, where $C = 1/\log(1/(2-\sqrt{3})) \approx 0.76$, we have

$$\min_{\alpha_1,\ldots,\alpha_m \in \mathbb{R}} L_{\text{Tik}}\left(\sum_i \alpha_i |u_i\rangle\right) \leqslant \min_{x \in \mathbb{C}^{2^n}} L_{\text{Tik}}(x) + \epsilon.$$

For example, when $\epsilon = 0.02$, we only need depth at most 4 and number of nodes $m \leqslant {K_A}^4$.

Proof. We show the argument for point (a) based on standard convex optimization results and refer to appendix E for the careful analysis of point (b). First, using that A is Hermitian, the gradient of the loss function is $\nabla L_{\text{Tik},\eta}(x) = \eta x + 2A^{\dagger}Ax - 2A^{\dagger}|b\rangle = \eta x + 2A^2 x - 2A|b\rangle$, and the Hessian is given by $\nabla^2 L_{\text{Tik},\eta}(x) = \eta \mathbb{1} + 2A^2$. Hence we have the bounds $\eta \mathbb{1} \preccurlyeq \nabla^2 L_{\text{Tik},\eta}(x) \preccurlyeq 3\mathbb{1}$ for all x. Performing a single gradient descent step with step size γ at the tth iteration yields the following relation $x^{(t+1)} \leftarrow x^{(t)} - \gamma(x^{(t)} + 2A^2 x^{(t)} - 2A|b\rangle)$. The step size γ can be determined by line search [48]. Suppose we start from $x^{(0)} = |b\rangle$, then after T iterations, the solution can be expressed as a polynomial $p(z)$ of degree T^2 of the matrix A applied to $|b\rangle$, i.e. $x^{(T)} = p(A)|b\rangle$, with well-defined polynomial coefficients. This polynomial directly expresses how to linearly combine the nodes in the ansatz tree up to depth T^2. From standard convex analysis [49] (section 9.3.1, in particular equation (9.19)), for strongly convex functions, if

$$T \geqslant \frac{\log((L_{\text{Tik},\eta}(|b\rangle) - \min_x L_{\text{Tik},\eta}(x))/\epsilon)}{\log(1/(1-\eta/3))} = \Theta\left(\frac{1}{\eta} \log(1/\epsilon)\right),$$

we have $L_{Tik,\eta}(x^{(T)}) - \min_x L_{Tik,\eta}(x) \leqslant \epsilon$. Hence, we have derived a required depth of $\mathcal{O}\left(\frac{1}{\eta^2} \log^2(1/\epsilon)\right)$. Using Newton's method this depth can be improved to $\mathcal{O}\left(\frac{1}{\eta} \log(1/\epsilon)\right)$. As we have to include a number of nodes exponential in the depth, the prefactor in the $\log 1/\epsilon$ dependency is crucial for near-term quantum

computing applications. Point (b) shows a favorable prefactor for the case of $\eta = 1$ using a more intricate proof (see appendix E). □

We summarize this result with a guarantee on the solution vector. Note that the optimal solutions x^* for propositions 4 and 5 are different. Obtaining a solution x close to the optimal solution x^* of the regularized linear system in proposition 5 can be easier and can require fewer resources.

Theorem 2 (Guarantee for solution to Tikhonov problem). *Let $|b\rangle$ and A be given as in assumptions 1 and 2. A solution x can be found with a guaranteed distance to the optimal solution $x^*_{T,\eta} = \arg\min_{x\in\mathbb{C}^{2^n}} L_{\mathrm{Tik},\eta}(x)$.*

(*a*) *For $\eta \in (0,1]$, the distance is $\left\|x - x^*_{T,\eta}\right\|_2^2 \leqslant \epsilon$ with high probability, using a per-measurement circuit depth $\mathcal{O}\left(\frac{1}{\eta}\log\left(\frac{1}{\eta\epsilon}\right)\right)$ and a basis set size of $\mathcal{O}\left(K_A^{\lceil \frac{1}{\eta}\log\left(\frac{1}{\eta\epsilon}\right)\rceil}\right)$.*

(*b*) *For $\eta = 1$, the distance is $\left\|x - x^*_{T,1}\right\|_2^2 \leqslant \epsilon$ with high probability, using a per-measurement circuit depth $\mathcal{O}\left(\log(1/\epsilon)\right)$, and a basis set size of $\mathcal{O}\left(K_A^{\lceil 0.76\ \log(1/\epsilon)\rceil}\right)$.*

Proof. The size of the basis set is determined by K_A exponentiated by the tree depth. Let $x = \sum_{i=1}^m \alpha_i |u_i\rangle$ for the optimal α_i minimizing $L_{\mathrm{Tik},\eta}\left(\sum_{i=1}^m \alpha_i |u_i\rangle\right)$. And let the optimal solution to $\min_{x\in\mathbb{C}^N} L_{\mathrm{Tik},\eta}(x)$ be $x^*_{T,\eta} = (A^2 + \eta/2)^{-1} A|b\rangle$. Using definition 2, we have

$$\epsilon \geqslant L_{\mathrm{Tik},\eta}(x) - L_{\mathrm{Tik},\eta}(x^*_{T,\eta}) = (x - x^*_{T,\eta})^\dagger \left(A^2 + \frac{\eta}{2}\right)(x - x^*_{T,\eta}) \geqslant \frac{\eta}{2}\left\|x - x^*_{T,\eta}\right\|_2^2. \tag{11}$$

Hence, the respective tree depth from proposition 5 suffices to find a solution $x = \sum_i \alpha_i |u_i\rangle$ close to the optimal solution x^* with $\left\|x - x^*_{T,\eta}\right\|_2^2 \leqslant \epsilon/\eta$. The required quantum resources are determined by the tree depth and, for point (b), independent of the condition number κ. □

Finally, we provide a connection of the solution of the Tikhonov regularized problem to the regression problem.

Proposition 6 *Fix $\epsilon > 0$ and $\eta > 0$. Let $|b\rangle$ and A be given as in assumptions 1 and 2. Let $x^*_R = \arg\min_{x\in\mathbb{C}^{2^n}} L_{\mathrm{Reg}}(x)$ and $x^*_{T,\eta} = \arg\min_{x\in\mathbb{C}^{2^n}} L_{\mathrm{Tik},\eta}(x)$. Let x_η be such that $L_{\mathrm{Tik},\eta}(x_\eta) \leqslant L_{\mathrm{Tik},\eta}(x^*_{T,\eta}) + \epsilon$ and $\|x^*_{T,\eta}\|_2^2 \leqslant \|x_\eta\|_2^2$. If*

$$\eta \leqslant \frac{L_{\mathrm{Reg}}(x^*_R) - L_{\mathrm{Reg}}(x^*_{T,\eta})}{\|x^*_{T,\eta}\|_2^2 - \|x_\eta\|_2^2}, \tag{12}$$

and if $\eta \in (0,1]$, then we obtain the desired guarantee for $L_{\mathrm{Reg}}(x_\eta)$.

Proof. Note that $L_{\mathrm{Reg}}(x^*_R) \leqslant L_{\mathrm{Reg}}(x^*_{T,\eta})$ and, by hypothesis, $\|x^*_{T,\eta}\|_2^2 \leqslant \|x_\eta\|_2^2$, and hence the stated bound for η is non-negative. We have,

$$L_{Reg}(x_\eta) = L_{\mathrm{Tik},\eta}(x_\eta) - \eta\|x_\eta\|_2^2 \leqslant L_{\mathrm{Tik},\eta}(x^*_{T,\eta}) - \eta\|x_\eta\|_2^2 + \epsilon. \tag{13}$$

If η is as given in the hypothesis then

$$L_{\mathrm{Tik},\eta}(x^*_{T,\eta}) - \eta\|x_\eta\|_2^2 = L_{\mathrm{Reg}}(x^*_{T,\eta}) + \eta\|x^*_{T,\eta}\|_2^2 - \eta\|x_\eta\|_2^2 \leqslant L_{\mathrm{Reg}}(x^*_R). \tag{14}$$

□

In practice, we may not know the quantities determining η in this proposition. We can use search on the interval $(0,1]$ to find η: start with $\eta = 1$, solve the Tikhonov problem, check if the solution satisfies the regression loss function bound. If not, then do the same for $\eta = \frac{1}{2}, \frac{1}{4}, \frac{1}{8}, \ldots$. For each η, this implies a tree depth via theorem 2. In some cases, this search may fail after a reasonable (say, constant) number of different η. We then output that a good η (that also solves the regression problem) does not exist within the resources we are willing to allocate. In this case, we cannot connect the Tikhonov solution to the regression solution.

4.5. Gradient expansion heuristics

Given the result of proposition 4 (two-norm regression), it is imperative to reduce the number of nodes considered in the optimization. Hence, we investigate methods which judiciously include nodes on the tree and prune branches which are not essential to the problem. We introduce a heuristic procedure for exploring the tree which we call the *gradient expansion heuristics*.

The key idea is to use the gradient information of the current state to expand the state space. Recall that the gradient with respect to the elements of x of the loss function is $\nabla_x L_{\mathrm{Reg}}(x) \equiv \nabla L_{\mathrm{Reg}}(x) = 2A^2x - 2A|b\rangle$.

Given a subspace S and an ansatz $x = \sum_{i\in S} \alpha_i |u_i\rangle$, consider the gradient with respect to α. We have $\nabla_\alpha L_{\text{Reg}}(\alpha) = 2V^2\alpha - 2q$, with the definitions of V and q as in section 4.2. Optimizing the coefficients $\alpha \to \alpha^*$ leads to a small gradient at the optimum $\nabla_\alpha L_{\text{Reg}}(\alpha^*) \approx 0$ and obtains a vector $x \to x'$. However, $\nabla L_{\text{Reg}}(x') \not\equiv 0$ in most cases as the subspace-optimized x' is not the optimum of $L_{\text{Reg}}(x)$. Hence we can use this gradient $\nabla L_{\text{Reg}}(x')$ to improve the subspace S, as described in the following.

At the start, let the subspace S contain only the root of the ansatz tree, i.e. $S = \{|b\rangle\}$. At each step, we perform the following steps.

(a) Solve for the optimal $x^S = \sum_{|u_i\rangle\in S} \alpha_i^* |u_i\rangle$ by optimizing over the combination parameters $\alpha_1, \ldots, \alpha_m$ as discussed in section 4.2.

(b) Let $\mathcal{C}(S)$ be the set of child nodes of the set S on the full ansatz tree. The size of the set is $|\mathcal{C}(S)| = K_A|S|$. For each quantum state $|u\rangle \in \mathcal{C}(S)$, compute the gradient overlap $\langle u| \nabla L_{\text{Reg}}(x^S) = 2\sum_{|u_i\rangle\in S} \alpha_i^* \langle u| A^2 |u_i\rangle - 2\langle u| A |b\rangle$. The overlaps $\langle u|u_i\rangle, \langle u| A |u_i\rangle, \langle u| A^2 |u_i\rangle$, for all $|u_i\rangle \in S$, can be computed efficiently using the Hadamard test via propositions 9 and 11.

(c) Add a new node to the subspace S, such that the node has the largest overlap with the gradient. More formally, select $|u^*\rangle = \arg\max_{|u\rangle\in\mathcal{C}(S)} |\langle u| \nabla L_{\text{Reg}}(x^S)|$ and grow the set $S \leftarrow S \cup \{|u^*\rangle\}$.

An illustration of this method can be found in figure 3. This gradient expansion procedure can be justified by the following proposition (see appendix E for the proof).

Proposition 7. *Consider a subspace S with m states $|u_1\rangle, \ldots, |u_m\rangle$, and the optimal $x^S = \sum_{|u_i\rangle\in S} \alpha_i^* |u_i\rangle$. If the gradient overlap of $|u^*\rangle$ is*

$$g = \left|\langle u^*| \nabla L_{\text{Reg}}(x^S)\right| = \left|2\sum_{|u_i\rangle\in S} \alpha_i^* \langle u^*| A^2 |u_i\rangle - 2\langle u^*| A |b\rangle\right| > 0,$$

then, after expanding the subspace $S \leftarrow S \cup \{|u^*\rangle\}$ and optimizing the combination parameters, the loss function will have a guaranteed decrease given by

$$\min_{\alpha_1,\ldots,\alpha_{m+1}\in\mathbb{C}} L_{\text{Reg}}\left(\sum_{|u_i\rangle\in S\cup\{|u^*\rangle\}} \alpha_i |u_i\rangle\right) \leqslant L_{\text{Reg}}\left(x^S\right) - \frac{g^2}{4}.$$

As a result of this proposition, if we find a new quantum state $|u^*\rangle$ with a nonzero gradient overlap, we are guaranteed that the next state vector $x^{S\cup\{|u^*\rangle\}}$ will be better than the current vector x^S. Furthermore, a larger gradient overlap guarantees a larger decrease in the loss function. Hence it is best to find a state vector that has the largest gradient overlap.

We now pinpoint limitations of the proposed ansatz tree CQS approach. The potential problems for variational algorithms discussed in section 3.4 do not apply to this ansatz tree CQS approach and the problematic linear systems could actually be solved easily. For the Tikhonov loss function, the CQS approach is also guaranteed to find a solution with near-optimal loss function in polynomial time. However, for the regression loss function, this approach is guaranteed to efficiently find the solution *only when* the condition number of A is bounded by a constant. Note that traditional quantum algorithms for linear systems [29, 47] are efficient for condition numbers that are polynomial in the number of qubits. When the condition number of A is too large, this ansatz tree CQS approach cannot guarantee to find the optimal solution in polynomial time. The gradient expansion heuristics can ameliorate this shortcoming in practice, but, in the worst case, it may still require an exponential amount of time when κ is too large.

4.6. Hamiltonian CQS approach and connection to previous results

The ansatz tree approach so far is based on the direct use of the decomposition of the matrix A, see assumption 2. As an alternative approach, one can generate a subspace by performing Hamiltonian simulation. Because of the use of Hamiltonian simulation, this approach is less near-term compared to using the ansatz tree. The benefit of this approach is that it greatly reduces the size of the ansatz subspace compared to proposition 4.

Reference [47] shows that the function $1/x$ can be well approximated by a Fourier series with near-optimal number of terms. This Fourier series can be viewed as a series for approximating $1/A$ and obtains a LCU of the form e^{-iAt_j} with pre-specified times t_j. Using a truncated Taylor method for quantum simulation of this linear combination [24] obtains a quantum state proportional to the exact solution $A^{-1}|b\rangle$. Based on reference [47] (lemma 11), we can choose the set of ansatz states as follows

$$\left\{|u_j\rangle := e^{-iAt_j}|b\rangle \,\middle|\, t_j = \frac{\epsilon j}{\kappa \log(\kappa/\epsilon)}, \quad j = -J, \ldots, J\right\}, \tag{15}$$

where $J = \Theta\left(\kappa^2 \log^2(\kappa/\epsilon)/\epsilon\right)$ and κ is an upper-bound on the condition number of A. This set is of size $2J + 1 = \Theta\left(\kappa^2 \log^2(\kappa/\epsilon)/\epsilon\right)$.

We make the following natural assumption for the simulation of e^{-iAt}. Such a simulation shall take a number of gates which scales linearly in the time, logarithmically in the accuracy, and linearly in some norm of A. For example, reference [24] showed a gate complexity of $\tilde{\mathcal{O}}\left(\|\beta\|_1 t\right)$ for a matrix of the form in assumption 2 via a truncated Taylor expansion, where $\|\beta\|_1$ is the ℓ_1-norm of the coefficient vector with elements β_k, and $\tilde{\mathcal{O}}(\cdot)$ suppresses all logarithmic factors.

We provide a statement about the circuit depth and the number of measurements.

Theorem 3 (Guarantee for solution to regression problem via Hamiltonian ansatz). *Let A and $|b\rangle$ be given as in assumptions 1 and 2. Also assume that the simulation of e^{-iAt} has a gate complexity of $\mathcal{O}(t)$. A solution x can be found such that the distance to the optimal solution $x^* = A^{-1}|b\rangle$ is*

$$\|x - x^*\|_2^2 \leqslant \epsilon \tag{16}$$

with high probability using a per-measurement circuit depth of

$$\mathcal{O}\left(\kappa \log(\kappa/\epsilon)\right) \tag{17}$$

and a basis set size of

$$\frac{\kappa^2 \log^2(\kappa/\epsilon)}{\epsilon}. \tag{18}$$

Proof. Using the CQS strategy, we are guaranteed to find an ϵ-close solution for $Ax = |b\rangle$ because of the Fourier approximation results of [47]. As discussed, $t_J = \mathcal{O}\left(\kappa \log(\kappa/\epsilon)\right)$ is the maximum simulation time for e^{-iAt}. A single run uses only a single ancilla for the Hadamard test, hence the overall single-run circuit depth is $\mathcal{O}\left(\kappa \log(\kappa/\epsilon)\right)$. The size of the basis set is the size of the set in equation (15), i.e. $\kappa^2 \log^2(\kappa/\epsilon)/\epsilon$. □

Recall that we never create the solution x on a quantum computer, and only store the combination coefficients classically. Hence, we avoid the need of more ancilla qubits in existing quantum algorithms based on function approximations [24, 47], at the cost of more measurements. We now compare this approach to the random-sampling approach taken in [29].

The approach in [29] eliminates the use of amplitude amplification and function approximation. In that work, the operators $e^{-iH(s_j)t_j}$ are used with the Hamiltonian from definition 3. The s_j are fixed via a natural parameterization and the t_j are randomly sampled from an interval of size about $[0, \mathcal{O}\left(\kappa^2\right)]$ for $j = 1, \ldots, \Theta\left(\log^2(\kappa)/\epsilon\right)$. The method is able to again achieve an ϵ-close approximation. The circuit depth is about $\mathcal{O}\left(\kappa \log(\kappa)/\epsilon\right)$, not counting details of the Hamiltonian simulation for $H(s)$. In comparison, the ansatz defined by the set in equation (15) shows the single-run circuit gate complexity of $\mathcal{O}\left(\kappa \log(\kappa/\epsilon)\right)$. This reduction in quantum resources comes at the cost of more classical repetitions. Hence, the Hamiltonian CQS approach fits into the general near-term strategy of trading the more expensive circuit depth for the cheaper number of runs of the experiments.

4.7. Numerical experiments

We now present numerical experiments for the linear system solvers using the ansatz tree approach. We do not consider the Hamiltonian CQS approach here due to the need of quantum simulation that makes the approach less near-term than the ansatz tree approach. In figure 4 (left), we compare the use of gradient expansion heuristics with the use of a breadth-first search that simply includes every node on the ansatz tree layer-by-layer. We consider randomly generated linear systems of size 256×256. We generate a random linear system by selecting several unitary matrices $U_1, \ldots, U_S$ from the Haar measure, random scalars $\alpha_1, \ldots, \alpha_S$ from uniform distribution $[-2, 2]$ and let $A = \sum_{i=1}^{S} \alpha_i (U_i + U_i^\dagger)$. This construction guarantees that A is Hermitian and is a weighted sum of unitary matrices. The condition number generated this way is very large (in the order of the system size). In particular, we consider $S = 10$ (hence A is a sum of 20 unitaries). A clear improvement can be seen when using the gradient expansion heuristics. With the use of this technique, rapid convergence to the optimal point is observed. On the other hand, a breath-first search, which layer by layer includes every node on the ansatz tree, results in a very slow convergence after an initial rapid convergence for 20 rounds (this includes the first layer of the ansatz tree).

In figure 4 (middle), we consider a special class of (sparse) linear systems that are extremely large. In particular, we consider system sizes ranging from $2^{10} \times 2^{10}$ to $2^{300} \times 2^{300}$ to investigate whether our new approach suffers from the plateau issue discussed in section 3.4. To facilitate classical simulation, we consider $A \in \mathbb{C}^{2^n \times 2^n}$ with efficient Pauli decomposition, i.e. $A = \sum_{i=1}^{S} \alpha_i P_1^{(i)} \otimes \cdots \otimes P_n^{(i)}$, where $P_j^{(i)}$ is a single-qubit Pauli operator (including the identity). In addition, we set $|b\rangle = |0^n\rangle$. To generate a random

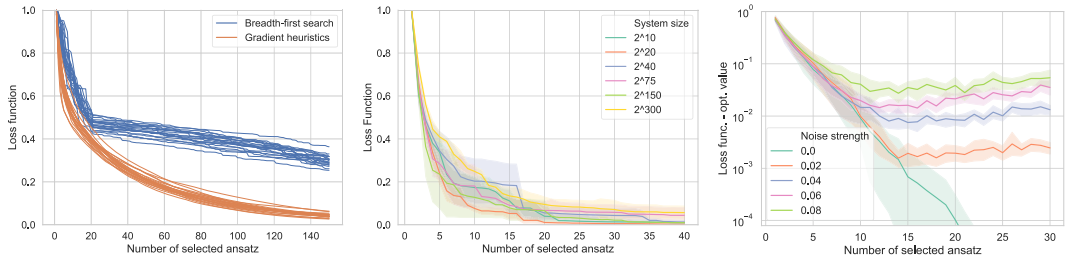

Figure 4. Numerical experiments on classical combination of quantum states algorithm for solving linear systems of equations. We use the standard loss function $L_{\mathrm{Reg}}(x) = \|Ax - b\|_2^2$. Left: comparison of breadth-first search and the gradient expansion heuristics for adding nodes on the ansatz tree to the subspace. We consider solving linear systems with a system size of 256×256 where A is generated by sampling random weighted sum of Haar-random unitaries. Matrices A generated this way have a large condition number (as large as the system size), so a large number of ansatz states are needed find the solution. Each line represents an independent run. Middle: solving linear systems over a wide range of system sizes (from $2^{10} \times 2^{10}$ to $2^{300} \times 2^{300}$). For efficient classical simulation, the linear systems are generated as random weighted sums of Pauli strings, i.e. tensor product of Pauli operators. The shaded areas represent the standard deviation over five independent runs. Right: testing the noise resilience of the proposed approach. We consider regularized linear systems (with L_{Tik} given in definition 2) generated as random weighted sums of Pauli strings with system size $2^{10} \times 2^{10}$. The noise strength represent the error obtained in each single entry of Q and r in the quadratic problem for solving the combination parameters, which could arise from decoherence, gate infidelity, or measurement error. The performance levels off or slightly degrades after certain number of ansatz due to the noise. The shaded areas represent the standard deviation over five independent runs.

matrix A, we sample each α_i from the uniform distribution over $[-2, 2]$, and a random tensor product of Pauli operators from the uniform distribution over 4^n possible choices. Here, we consider $S = 8$. Note that when $S = 1$ and we only sample from I or X in the Pauli string, then we recover the toy problem that leads to the plateau issues discussed in section 3.4. From figure 4, we can see that this approach circumvents the plateau issue and has a clear convergence over a remarkably wide range of system sizes.

In figure 4 (right), we consider solving regularized (sparse) linear systems under the effect of noise. We consider the same procedure for generating the matrix A and vector $|b\rangle$. Our approach relies on optimization of m combination parameters for the selected ansatz: $\min_z z^T Q z - 2r^T z + 1$, which depends on $Q \in \mathbb{R}^{2m \times 2m}$ and $r \in \mathbb{R}^{2m}$ discussed in section 4.2. We can use the modified Hadamard test to estimate these quantities (see proposition 11). However, there will be errors coming from decoherence, gate infidelity, and quantum measurements. We consider every entry of Q and r to have errors, which we model by a Gaussian noise of varying standard deviation (up to 0.08). Note that when we have selected 30 ansatz states, all the 60×60 entries in Q will be subject to errors of strength up to 0.08. Together, this amounts to a rather large error (a naive bound gives $3600 * 0.08 = 288$). However, we found that even with such a large error, one can still achieve a good solution (in terms of loss function).

5. Discussion

This work provides algorithms for solving linear systems on near-term quantum computers. The input model is one of a LCU. Recent works discusses randomized classical algorithms for low-rank matrices [50], inspired by quantum algorithms in the context of linear algebra and machine learning. For these methods, one is given an importance sampling data structure for the matrix and achieves a dimension-efficient time complexity, but obtains substantial dependence on the error and other parameters. To our knowledge, there have been no studies on the LCU model in this context.

The flavor of the presented algorithms is two-fold. The first set of algorithms are variational in nature and draw their inspiration from other variational quantum algorithms for quantum chemistry [18, 42, 51, 52] and quantum optimization [21, 53, 54]. For such algorithms, the quantum computer implements a single wavefunction ansatz which is dependent on a set of variational parameters, usually in a non-linear fashion. The type of ansatz in this setting can, in the extreme cases, be linear system-independent (agnostic) or fully linear system-dependent. As the agnostic case is useful for example when limitations of the hardware are dominating the overall implementation, such ansätze have also been called 'hardware efficient' [20]. On the other hand, the dependent ansatz takes into account the linear system at the cost of requiring Hamiltonian simulation which increases the overall complexity of implementing such an ansatz in a near-term quantum processor. We exhibit types of linear systems for which variational approaches with a polynomial number of variational parameters show ill-shaped optimization landscape with plateaus and local minima. These issues may however not arise for other types of linear systems and ansätze with more structure and when using different loss functions. An important

future work is to better characterize those linear systems where variational methods offer near-term quantum advantages.

The second set of approaches are based on CQS. Here, we have used the two-norm regression and Tikhonov loss functions, which in general obtain different solutions to the linear system. The CQS method introduces a new set of combination parameters to add together different ansatz quantum states. The combination is emulated classically rather than represented directly on the quantum computer. Hence, the method increases the overall expressiveness and power of the total ansatz without the need of additional quantum resources. The CQS method can employ variational states such as the ones presented in the first part of this work and others yet to be developed, and non-variational states. Our CQS approach is also reminiscent of techniques used for example in quantum chemistry, where the linear combination of atomic orbitals approach allows to optimally construct molecular orbitals from atomic orbitals. To avoid optimizing variational parameters, we have proposed an approach that alternates between solving for the optimal solution in a subspace and growing the subspace on an ansatz tree. This approach is inspired by the Krylov subspace method in solving linear systems. The ansatz tree is also reminiscent of the coupled-cluster ansatz in quantum chemistry [55–58], which systematically takes into account higher orders of the electron correlation at the cost of increasing the complexity of preparing the ansatz.

We have performed numerical experiments solving exponentially large linear systems with sizes up to $2^{300} \times 2^{300}$. These experiments are achieved by considering a special class of linear systems that allows efficient simulation of the proposed quantum algorithm on a classical computer. To achieve actual quantum advantage, we require either A to be a sum of unitaries that cannot be simulated efficiently on a classical computer or b to be a quantum state generated by some quantum circuit. It should be noted that there will always be a trade-off between how near-term the quantum algorithm is (the required quantum coherence, entanglement, and interference) and how much quantum advantage we can expect from executing the quantum algorithm. An important future direction would be a detailed analysis on the performance of the proposed algorithms under the effect of decoherence and imperfections of real-world quantum devices. We believe the synthesis and future improvement of the proposed ideas can provide real benefits for solving linear systems on nearer-term quantum computers.

Acknowledgments

We would like to thank Fernando Brandao, Yudong Cao, Richard Kueng, John Preskill, Ansis Rosmanis, Miklos Santha, Thomas Vidick, and Zhikuan Zhao for valuable discussions. HH is supported by the Kortschak Scholars Program and thanks the hospitality of the Centre for Quantum Technologies. KB acknowledges the CQT Graduate Scholarship. PR acknowledges support from the Singapore National Research Foundation, the Prime Minister's Office, Singapore, the Ministry of Education, Singapore under the Research Centres of Excellence programme under research Grant No. R 710-000-012-135, and Baidu-NUS Research Project No. 2019-03-07.

Conflict of interests

The authors declare no competing financial or non-financial interests.

Data availability

The data that support the findings of this study are available upon reasonable request from the authors.

Author contribution

All authors contributed to the research conducted in this work and the writing of the manuscript. KB performed the numerical calculations for the variational method. HH performed the numerical calculations for the CQS approach.

Appendix A. Measurements

Lemma 1. *Let $\epsilon > 0$ and P_k be a certain Pauli string over n qubits. Let multiple copies of an arbitrary n-qubit quantum state $|\psi\rangle$ be given. The expectation value $\langle\psi| P_k |\psi\rangle$ can be determined to additive accuracy ϵ with failure probability at most δ using $\mathcal{O}\left(\frac{1}{\epsilon^2}\log(\frac{1}{\delta})\right)$ copies of $|\psi\rangle$.*

Proof. A single measurement obtains the outcome $m_\pm = \pm 1$. We have $\langle\psi| P_k |\psi\rangle = pm_+ + (1-p)m_- = 2p-1$, where p is the probability of measuring $+1$. To estimate this probability, perform independent trials of the Bernoulli test. Each trial has expectation value p. We use the statistic M_+/M, where M_+ is the number of positive outcomes over M trials. For the error estimate, we require $P\left[\left|2M_+/M - 1 - \langle\psi| P_k |\psi\rangle\right| \geqslant \epsilon\right] \leqslant \delta$ from which the number of measurements is $\mathcal{O}\left(\frac{1}{\epsilon^2}\log(\frac{1}{\delta})\right)$ via Hoeffding's inequality. □

Proposition 8 (Swap test). *Given multiple copies of n-qubit quantum states $|u\rangle$ and $|v\rangle$. There is a quantum algorithm that determines the overlap $|\langle v|u\rangle|^2$ to additive accuracy ϵ with failure probability at most δ using $\mathcal{O}\left(\frac{1}{\epsilon^2}\log(\frac{1}{\delta})\right)$ copies and $\tilde{\mathcal{O}}\left(\frac{1}{\epsilon^2}\log(\frac{1}{\delta})\right)$ operations.*

Proof. Use an ancilla and perform a controlled swap $\frac{1}{\sqrt{2}}\left(|0\rangle + |1\rangle\right)|u\rangle|v\rangle \to \frac{1}{\sqrt{2}}\left(|0\rangle|u\rangle|v\rangle + |1\rangle|v\rangle|u\rangle\right)$. Performing a Hadamard on the ancilla obtains $\frac{1}{2}\left(|0\rangle\left(|u\rangle|v\rangle + |v\rangle|u\rangle\right) + |1\rangle\left(|u\rangle|v\rangle - |v\rangle|u\rangle\right)\right) =: |\xi\rangle$. Now measure the ancilla in Z. The expectation value is $\langle\xi| Z |\xi\rangle = \frac{1}{4}\left(\langle u|\langle v| + \langle v|\langle u|\right)\left(|u\rangle|v\rangle + |v\rangle|u\rangle\right) - \frac{1}{4}\left(\langle u|\langle v| - \langle v|\langle u|\right)\left(|u\rangle|v\rangle - |v\rangle|u\rangle\right) = |\langle v|u\rangle|^2$. □

We can also measure the real and imaginary part separately under a different input model.

Proposition 9 (Hadamard test). *Assume the controlled state preparation $U_{prep} = |0\rangle\langle 0| \otimes U_{v_0} + |1\rangle\langle 1| \otimes U_{v_1}$, with $U_{v_j}|0^n\rangle = |v_j\rangle$. There is a quantum algorithm that determines $\mathrm{Re}\{\langle v_0|v_1\rangle\}$ and $\mathrm{Im}\{\langle v_0|v_1\rangle\}$ to additive accuracy ϵ with failure probability at most δ using $\mathcal{O}\left(\frac{1}{\epsilon^2}\log(\frac{1}{\delta})\right)$ applications of U_{prep} and $\tilde{\mathcal{O}}\left(\frac{1}{\epsilon^2}\log(\frac{1}{\delta})\right)$ operations.*

Proof. Use an ancilla prepared in $(|0\rangle + \alpha|1\rangle)/\sqrt{2}$ with $\alpha = 1$ or $\alpha = i$. Apply U_{prep} to obtain $\frac{1}{\sqrt{2}}\left(|0\rangle|v_0\rangle + \alpha|1\rangle|v_1\rangle\right)$. Another Hadamard on the ancilla obtains $\frac{1}{2}\left(|0\rangle\left(|v_0\rangle + \alpha|v_1\rangle\right) + |1\rangle\left(|v_0\rangle - \alpha|v_1\rangle\right)\right) =: |\xi\rangle$. Now measure the ancilla in Z. The expectation value is $\langle\xi| Z |\xi\rangle = \frac{1}{2}\left(\alpha\langle v_0|v_1\rangle + \alpha^*\langle v_1|v_0\rangle\right)$. If $\alpha = 1$, then $\langle\xi| Z |\xi\rangle = \mathrm{Re}\{\langle v_0|v_1\rangle\}$. If $\alpha = i$, then $\langle\xi| Z |\xi\rangle = \mathrm{Im}\{\langle v_0|v_1\rangle\}$. □

Proposition 10 (Measuring the Hamiltonian loss function). *Given assumption 2 on the unitary decomposition of A and multiple copies of the quantum state $|x\rangle$. The loss function $\langle x| A^2 |x\rangle - \langle x| A |b\rangle\langle b| A |x\rangle$ can be estimated efficiently on a quantum computer. More precisely, an estimate up to additive error ϵ can be obtained with probability $1-\delta$ using $\mathcal{O}\left(\frac{(\sum_k|\beta_k|)^4}{\epsilon^2}\log\frac{K_A}{\delta}\right)$ quantum measurements.*

Proof. From definition 2, define the size parameter $\eta = \sum_{k,l}|\beta_k\beta_l|$. The first term of the loss function is $A^2 = \sum_k\sum_l \beta_k\beta_l U_k U_l$. Measure each term $\langle x| U_k U_l |x\rangle$ individually using the Hadamard test in proposition 9 with $|v_0\rangle = |x\rangle$ and $|v_1\rangle = U_k U_l |x\rangle$. For each term, perform $\mathcal{O}\left(\frac{|\beta_k\beta_l|\eta}{\epsilon^2}\log\frac{K_A}{\delta}\right)$ quantum measurements to produce an estimate $\langle x|\widetilde{U_k U_l}|x\rangle$ of $\langle x| U_k U_l |x\rangle$ up to additive accuracy $\epsilon/\sqrt{\eta|\beta_k\beta_l|}$ with success probability $1 - \frac{\delta}{2K_A^2}$. Thus the additive accuracy for the estimate $\langle x|\widetilde{A^2}|x\rangle$ of $\langle x| A^2 |x\rangle$ is $\left|\langle x|\widetilde{A^2}|x\rangle - \langle x| A^2 |x\rangle\right| \leqslant \epsilon$, which is obtained by adding up the variances of each independent estimate scaled by the coefficients $|\beta_k\beta_l|^2$ and taking the square root. The total success probability is $\left(1 - \frac{\delta}{2K_A^2}\right)^{K_A^2} \geqslant \mathrm{e}^{-\delta} \geqslant 1-\delta$. The total number of measurements is $\mathcal{O}\left(\frac{\sum_{kl}|\beta_k\beta_l|\eta}{\epsilon^2}\log\frac{K_A}{\delta}\right) = \mathcal{O}\left(\frac{(\sum_k|\beta_k|)^4}{\epsilon^2}\log\frac{K_A}{\delta}\right)$.

For the second term, with $A = \sum_k \beta_k U_k$ estimate $\langle b| A |x\rangle = \sum_k \beta_k \langle b| U_k |x\rangle$. Use the Hadamard test in proposition 9 with $|v_0\rangle = |b\rangle$ and $|v_1\rangle = U_k |x\rangle$ to estimate each term $\langle b| U_k |x\rangle$. For each term, perform $\mathcal{O}\left(\frac{|\beta_k|(\sum_{k'}|\beta_{k'}|)^3}{\epsilon^2}\log\frac{K_A}{\delta}\right)$ quantum measurements to estimate $\langle b| U_k |x\rangle$ up to variance $\epsilon^2/\left(|\beta_k|\left(\sum_{k'}|\beta_{k'}|\right)^3\right)$ with success probability $1 - \frac{\delta}{8K_A}$. Thus the variance in the estimation of $\langle b| A |x\rangle$ is $\epsilon^2/(\sum_{k'}|\beta_{k'}|)^2$ with success probability $1 - \frac{\delta}{4}$ using a total of $\mathcal{O}\left(\frac{(\sum_k|\beta_k|)^4}{\epsilon^2}\log\frac{K_A}{\delta}\right)$ quantum measurements. The term $\langle x| A |b\rangle\langle b| A |x\rangle$ can be estimated by performing two independent estimations of $\langle x| A |b\rangle$ and $\langle b| A |x\rangle$ and multiplying them together. The variance of $\langle x| A |b\rangle\langle b| A |x\rangle$ is $2|\langle x| A |b\rangle|^2 \mathrm{Var}[\langle b| A |x\rangle] + \mathrm{Var}[\langle b| A |x\rangle]^2$ which is bounded by $4|\langle x| A |b\rangle|^2 \mathrm{Var}[\langle b| A |x\rangle] \leqslant 4\left(\sum_k|\beta_k|\right)^2 \cdot \epsilon^2/\left(\sum_k|\beta_k|\right)^2 = 4\epsilon^2$ with success probability $1-\delta$ and uses a total of $\mathcal{O}\left(\frac{(\sum_k|\beta_k|)^4}{\epsilon^2}\log\frac{K_A}{\delta}\right)$ quantum measurements.

Summing over the first and the second term obtains an estimation for the loss function with variance $5\epsilon^2$. By considering $\epsilon \leftarrow \epsilon/\sqrt{5}$ and $\delta \leftarrow \delta/4$, an estimation for the loss function with variance ϵ^2 and success probability $1-\delta$ is obtained using $\mathcal{O}\left(\frac{(\sum_k|\beta_k|)^4}{\epsilon^2}\log\frac{K_A}{\delta}\right)$ quantum measurements. □

Proposition 11 (Modified Hadamard test for bounded observables). *Assume the controlled state preparation* $U_{prep} = |0\rangle\langle 0| \otimes U_{v_0} + |1\rangle\langle 1| \otimes U_{v_1}$, *with* $U_{v_j}|0^n\rangle = |v_j\rangle$ *is an n-qubit state. Given an observable* $O = U^\dagger DU \in \mathbb{C}^{2^n \times 2^n}$, *where U is a unitary matrix that can be implemented efficiently as a quantum circuit, D is a real diagonal matrix, and* D_{ii} *can be computed efficiently as a classical function* $f: [2^n] \to [-1, 1]$. *Both* $\mathrm{Re}\{\langle v_0| O |v_1\rangle\}$ *and* $\mathrm{Im}\{\langle v_0| O |v_1\rangle\}$ *can be estimated efficiently on a quantum computer. More precisely, we can estimate* $\mathrm{Re}\{\langle v_0| O |v_1\rangle\}$ *and* $\mathrm{Im}\{\langle v_0| O |v_1\rangle\}$ *to additive accuracy* ϵ *with failure probability at most* δ *using* $\mathcal{O}\left(\frac{1}{\epsilon^2}\log(\frac{1}{\delta})\right)$ *quantum measurements.*

Proof. Use an ancilla prepared in $\left(|0\rangle + \alpha|1\rangle\right)/\sqrt{2}$ with $\alpha = 1$ or $\alpha = i$. Apply UU_{prep} to obtain $\frac{1}{\sqrt{2}}\left(|0\rangle \otimes U|v_0\rangle + \alpha|1\rangle \otimes U|v_1\rangle\right)$. Another Hadamard on the ancilla gives $|\xi\rangle = \frac{1}{2}(I \otimes U)$ $\left(|0\rangle(|v_0\rangle + \alpha|v_1\rangle) + |1\rangle(|v_0\rangle - \alpha|v_1\rangle)\right)$. Now measure the ancilla in Z to obtain $z_a \in \{\pm 1\}$ and the rest of the state in the computational basis to obtain $b \in \{0,1\}^n$. Then compute $z_a f(b)$. The expectation value is $\langle\xi| Z \otimes D |\xi\rangle = \frac{1}{2}\left(\alpha\langle v_0| O |v_1\rangle + \alpha^*\langle v_1| O |v_0\rangle\right)$. If $\alpha = 1$, then $\langle\xi| Z \otimes D |\xi\rangle = \mathrm{Re}\{\langle v_0| O |v_1\rangle\}$. If $\alpha = i$, then $\langle\xi| Z \otimes D |\xi\rangle = \mathrm{Im}\langle v_0| O |v_1\rangle$. Because each sample $z_a f(b)$ is between -1 and 1, Hoeffding's inequality shows that taking the average of $\mathcal{O}\left(\frac{1}{\epsilon^2}\log(\frac{1}{\delta})\right)$ samples results in an estimate within error at most ϵ with probability at least $1 - \frac{1}{\delta}$. □

Appendix B. Plateau for simple randomized linear systems

Proof of proposition 1. Let the distribution over the random matrix A be

$$A = (\sigma_x^{(1)})^{k_1} \otimes \cdots \otimes (\sigma_x^{(n)})^{k_n}, \tag{B1}$$

where $k \in \{0,1\}^n$ is a uniformly random n-bit string. For $\|A|x(\theta)\rangle - |b\rangle\|_2^2$ from definition 1, the gradient at an initial point θ^0 is

$$\frac{\partial}{\partial\theta_i}\|A|x(\theta)\rangle - |b\rangle\|_2^2 = -2\,\mathrm{Re}\left\{\langle b| A\frac{\partial}{\partial\theta_i}|x(\theta^0)\rangle\right\}. \tag{B2}$$

Let us define the two-norm of the partial derivative,

$$\left\|\frac{\partial}{\partial\theta_i}|x(\theta^0)\rangle\right\| = G. \tag{B3}$$

Because the norm of $\frac{\partial}{\partial\theta_i}|x(\theta^0)\rangle$ is equal to G, we can see that there are at most $2^{n/2}$ entries in $\frac{\partial}{\partial\theta_i}|x(\theta^0)\rangle$ with squared absolute value $\geqslant G^2/2^{n/2}$.

Recall that $A|b\rangle = |k\rangle$ where $k \in \{0,1\}^n$ due to the distribution over the random matrix A. So the probability that the following event happens

$$\left|\langle b| A\frac{\partial}{\partial\theta_i}|x(\theta^0)\rangle\right|^2 \geqslant G^2/2^{n/2} \tag{B4}$$

is at most $1/2^{n/2}$. By union bound, with probability at least $1 - m/2^{n/2}$, we will have

$$\left|\langle b| A\frac{\partial}{\partial\theta_i}|x(\theta^0)\rangle\right|^2 < G^2/2^{n/2}, \quad \forall\, i = 1,\ldots,m. \tag{B5}$$

Hence we have the following statement

$$\left|\frac{\partial}{\partial\theta_i}\|A|x(\theta)\rangle - |b\rangle\|_2^2\Big|_{\theta=\theta^0}\right|^2 \leqslant 4\left|\langle b| A\frac{\partial}{\partial\theta_i}|x(\theta^0)\rangle\right|^2 < 4G^2/2^{n/2}, \quad \forall\, i = 1,\ldots,m, \tag{B6}$$

with probability at least $1 - \frac{m}{2^{n/2}}$. Together, we have

$$\left|\frac{\partial}{\partial\theta_i}\|A|x(\theta)\rangle - |b\rangle\|_2^2\Big|_{\theta=\theta^0}\right| \leqslant \frac{2}{2^{n/4}}\left\|\frac{\partial}{\partial\theta_i}|x(\theta)\rangle\right\|, \quad \forall\, i = 1,\ldots,m, \tag{B7}$$

with probability at least $1 - m/2^{n/2}$.

The analysis is analogous for $\langle x(\theta)|(A^2 - A|b\rangle\langle b|A)|x(\theta)\rangle$ from definition 4. Pick an initial point θ^0, the partial derivative at an initial point θ^0 is

$$\frac{\partial}{\partial\theta_i}\langle x(\theta)|(A^2 - A|b\rangle\langle b|A)|x(\theta)\rangle = -2\,\mathrm{Re}\left\{\langle x(\theta^0)|A|b\rangle\langle b|A\frac{\partial}{\partial\theta_i}|x(\theta^0)\rangle\right\}. \tag{B8}$$

We have that with probability at least $1 - m/2^{n/2}$,

$$\left|\langle b| A \frac{\partial}{\partial \theta_i} |x(\theta^0)\rangle\right|^2 < G^2/2^{n/2}, \quad \forall\, i = 1, \ldots, m, \tag{B9}$$

from the analysis before; see equation (B5). Furthermore,

$$\left|\langle x(\theta^0)| A |b\rangle\right| = \left|\langle x(\theta^0)| |k\rangle\right| \leqslant 1. \tag{B10}$$

Recall the definition that $G = \left\| \frac{\partial}{\partial \theta_i} |x(\theta)\rangle \right\|$, we have

$$\left| \frac{\partial}{\partial \theta_i} \langle x(\theta)| (A^2 - A |b\rangle \langle b| A) |x(\theta)\rangle \Big|_{\theta=\theta^0} \right| \leqslant \frac{2}{2^{n/4}} \left\| \frac{\partial}{\partial \theta_i} |x(\theta)\rangle \right\|, \quad \forall\, i = 1 \ldots, m, \tag{B11}$$

This concludes the proof of this proposition. □

An intuitive view on the plateau illustrated in the above proposition is that a rank-1 projection, such as $\langle x(\theta)| A |b\rangle \langle b| A |x(\theta)\rangle$ in the Hamiltonian loss function, is exponentially small, hence gives insignificant signal on how to find the solution. In [30, 59, 60], another type of loss function, called the local loss function, has been defined to ameliorate this problem. In the context of linear systems, it is defined as $\langle x(\theta)| A U_b (\mathbb{1} - \frac{1}{n}\sum_i |0_i\rangle \langle 0_i|) U_b^\dagger A |x(\theta)\rangle$, where U_b is the circuit to generate the state $|b\rangle$ and $|0_i\rangle \langle 0_i|$ is the projection onto the ith qubit. Intuitively, this prevents the projection from being exponentially small because it is now a sum of single qubit projections. When $U_b = \mathbb{1}$, and $A = (\sigma_x^{(1)})^{k_1} \otimes \cdots \otimes (\sigma_x^{(n)})^{k_n}$, this local loss function could indeed provide sufficient signal to solve the problem. However, a similar plateau problem may appear in cases where A and U_b contain many entangling circuits. In appendix C, we will show that when A and U_b are random polynomial-sized quantum circuits, the local loss function plateaus at the value $1/2$. The basic idea is that the single-qubit reduced density matrix of an entangled quantum state will be very close to a completely mixed state. Even though single qubit projection $|0_i\rangle \langle 0_i|$ will not be exponentially small, it will be sharply concentrated at the value $1/2$ with an exponentially small variance. While the local loss function would have a flat landscape when A and $|b\rangle$ are based on polynomial-sized quantum circuits sampled randomly, if A and $|b\rangle$ have more structure the local loss function can provide benefits for the variation optimization [30, 59, 60].

Appendix C. Potential problems for local loss function in the presence of entangling gates

Consider the case where $A \in \mathbb{C}^{2^n \times 2^n}$ is Hermitian and unitary (equivalently, all eigenvalue of A are 1 or -1) and $|b\rangle = U_b |0^n\rangle$. And let $|x(\theta)\rangle$ be some pre-specified ansatz with variational parameter θ. We now analyze the local loss function

$$L_L(\theta) = \langle x(\theta)| A U_b \left(\mathbb{1} - \frac{1}{n}\sum_{i=1}^n |0_i\rangle \langle 0_i| \right) U_b^\dagger A |x(\theta)\rangle = 1 - \frac{1}{n}\sum_{i=1}^n \langle x(\theta)| A U_b |0_i\rangle \langle 0_i| U_b^\dagger A |x(\theta)\rangle .$$

When U_b is a random quantum circuit consisting of $\mathcal{O}(n^2)$ 1D nearest neighbor two-qubit gates [61], shows that for any quantum state $|x(\theta)\rangle$, the two-design property of the random unitary $U_b^\dagger$ gives

$$\left\| \mathbb{E}_{U_b, A} \left[(U_b^\dagger A |x(\theta)\rangle \langle x(\theta)| A U_b)^{\otimes 2} \right] - \frac{\mathbb{1} + S}{(2^n + 1)2^n} \right\|_1 \leqslant \frac{1}{2^{n^2}}, \tag{C1}$$

where S is the swap operator and $\|\cdot\|_1$ is the trace norm. Let $R_i = \langle x(\theta)| A U_b |0_i\rangle \langle 0_i| U_b^\dagger A |x(\theta)\rangle$ be a random variable. Then using $\frac{1}{2} = \frac{1}{2} \langle x(\theta)| A U_b (|0_i\rangle \langle 0_i| + |1_i\rangle \langle 1_i|) U_b^\dagger A |x(\theta)\rangle$, we have

$$R_i - \frac{1}{2} = \frac{1}{2} \langle x(\theta)| A U_b (|0_i\rangle \langle 0_i| - |1_i\rangle \langle 1_i|) U_b^\dagger A |x(\theta)\rangle = \frac{1}{2} \langle x(\theta)| A U_b Z_i U_b^\dagger A |x(\theta)\rangle ,$$

where Z_i is the Pauli Z operator on the ith qubit. Hence by Markov's inequality,

$$\mathbb{P}\left[\left| R_i - \frac{1}{2} \right| > \frac{1}{2^{n/4}} \right] \leqslant 2^{n/2} \mathbb{E} \left[\left| R_i - \frac{1}{2} \right|^2 \right] \tag{C2}$$

$$= \frac{1}{4} 2^{n/2} \operatorname{Tr} \left(Z_i^{\otimes 2} \mathbb{E}_{U_b, A} \left[(U_b^\dagger A |x(\theta)\rangle \langle x(\theta)| A U_b)^{\otimes 2} \right] \right). \tag{C3}$$

For any linear operator P, Q and Q', we have

$$|\operatorname{Tr}(PQ) - \operatorname{Tr}(PQ')| \leqslant \|P\|_\infty \|Q - Q'\|_1 \;\Rightarrow\; \operatorname{Tr}(PQ) \leqslant \operatorname{Tr}(PQ') + \|P\|_\infty \|Q - Q'\|_1. \tag{C4}$$

Combining inequality (C1) and (C4), we have

$$\operatorname{Tr}\left(Z_i^{\otimes 2} \mathbb{E}_{U_b,A}\left[(U_b^\dagger A |x(\theta)\rangle \langle x(\theta)| AU_b)^{\otimes 2}\right]\right) \leqslant \operatorname{Tr}\left(Z_i^{\otimes 2} \frac{\mathbb{1} + S}{(2^n+1)2^n}\right) + \frac{1}{2^{n^2}} = \frac{1}{2^n} + \frac{1}{2^{n^2}}.$$

Now putting this result back to the Markov's inequality in (C2), we have

$$\mathbb{P}\left[\left|R_i - \frac{1}{2}\right| > \frac{1}{2^{n/4}}\right] \leqslant \frac{1}{4}\left(\frac{1}{2^{n/2}} + \frac{1}{2^{n^2-n/2}}\right) \leqslant \frac{1}{2^{n/2}}.$$

Using union bound and the definition of the local loss function, we have

$$\left|L_L(\theta) - \frac{1}{2}\right| \leqslant \frac{1}{2^{n/4}},$$

with probability at least $1 - n/2^{n/2}$. Hence, for any $\theta_1, \ldots, \theta_M$ (there can be an exponential number of them, i.e. $M \leqslant \frac{2^{n/2}}{50n}$),

$$\left|L_L(\theta_i) - \frac{1}{2}\right| \leqslant \frac{1}{2^{n/4}}, \quad \forall\, i = 1, \ldots, M,$$

with probability at least 0.98. This means that even if we randomly select a very large number of variational parameters, the local loss function will still be exponentially close to the value $1/2$ for all of them.

Now, consider a local expansion of $L_L(\theta)$ around θ^0,

$$1 - \frac{1}{n}\sum_{i=1}^{n}\left(\langle x(\theta^0)| AU_b |0_i\rangle \langle 0_i| U_b^\dagger A |x(\theta^0)\rangle\right. \tag{C5}$$

$$\left. - \sum_{k=1}^{m} 2\,\mathrm{Re}\left\{\langle x(\theta^0)| AU_b |0_i\rangle \langle 0_i| U_b^\dagger A \frac{\partial}{\partial\theta_k} |x(\theta^0)\rangle\right\} \delta\theta_k\right) + \mathcal{O}\left(m^2 \delta\theta_i^2\right). \tag{C6}$$

We analyze the partial derivative of the loss function in θ_k. We consider the random variable $g_k = 2\,\mathrm{Re}\left\{\langle x(\theta^0)| AU_b |0_i\rangle \langle 0_i| U_b^\dagger A \frac{\partial}{\partial\theta_k} |x(\theta^0)\rangle\right\}$, and define $u = |x(\theta^0)\rangle$ and $v = \frac{\partial}{\partial\theta_k} |x(\theta^0)\rangle$. We assume that $\|v\| = \left\|\frac{\partial}{\partial\theta_k} |x(\theta^0)\rangle\right\| \leqslant C$, for some constant C, which is true when the variational parameters are single-qubit rotation angles. The random variable g_k could be written as

$$g_k = \operatorname{Tr}\left(\left(vu^\dagger + uv^\dagger\right) AU_b |0_i\rangle \langle 0_i| U_b^\dagger A\right). \tag{C7}$$

We first note that the normalization condition of quantum states $\langle x(\theta)|x(\theta)\rangle = 1$ implies that $\frac{\partial}{\partial\theta_k} \langle x(\theta)| |x(\theta)\rangle = u^\dagger v + v^\dagger u = 0$. Using the results in [61], the two-design property of the random unitary U_b gives

$$\left\|\mathbb{E}_{U_b,A}\left[(AU_b |0_i\rangle \langle 0_i| U_b^\dagger A)^{\otimes 2}\right] - \frac{(2^{2n-2} - 2^{-1})\mathbb{1} + (2^{n-1} - 2^{n-2})S}{2^{2n} - 1}\right\|_1 \leqslant \frac{1}{2^{n^2}}. \tag{C8}$$

Now we bound the second moment of the random variable g_k,

$$\begin{aligned}
\mathbb{E}_{U_b,A}\left[g_k^2\right] &= \operatorname{Tr}\left(\left(vu^\dagger + uv^\dagger\right)^{\otimes 2} \mathbb{E}_{U_b,A}\left[(AU_b |0_i\rangle \langle 0_i| U_b^\dagger A)^{\otimes 2}\right]\right) \\
&\leqslant \operatorname{Tr}\left(\left(vu^\dagger + uv^\dagger\right)^{\otimes 2} \frac{(2^{2n-2} - 2^{-1})\mathbb{1} + (2^{n-1} - 2^{n-2})S}{2^{2n} - 1}\right) + \frac{1}{2^{n^2}}\left\|\left(vu^\dagger + uv^\dagger\right)^{\otimes 2}\right\|_\infty, \\
&= \frac{2^{n-1} - 2^{n-2}}{2^{2n} - 1} \operatorname{Tr}\left(\left(vu^\dagger + uv^\dagger\right)^{\otimes 2} S\right) + \frac{1}{2^{n^2}}\left\|\left(vu^\dagger + uv^\dagger\right)^{\otimes 2}\right\|_\infty, \\
&\leqslant \frac{2^{n-1} - 2^{n-2}}{2^{2n} - 1} 4C^2 + \frac{1}{2^{n^2}} 4C^2 \leqslant \frac{8C^2}{2^n}.
\end{aligned}$$

The first line uses equation (C7), and the second line uses inequality (C4) and (C8). The third line uses the fact that $u^\dagger v + v^\dagger u = 0$, while the last line uses the fact that $\|v\| \leqslant C$. Again by Markov's inequality, we have

$$\mathbb{P}\left[|g_k| > \frac{2C}{2^{n/4}}\right] \leqslant \frac{2^{n/2}\mathbb{E}_{U_b,A}\left[g_k^2\right]}{4C^2} \leqslant \frac{2}{2^{n/2}}.$$

Thus given $m \ll 2^{n/2}$, union bound on the above result gives

$$|g_k| \leqslant \frac{2C}{2^{n/4}}, \quad \forall\ k = 1, \ldots, m,$$

with high probability (more precisely, with probability $\geqslant 1 - 2m/2^{n/2}$). This means that the gradient would be exponentially small and the optimization landscape is locally flat around θ^0. From the analysis, we can see that the local loss function $L_L(\theta)$ will plateau at the value $1/2$ with an exponentially small deviation at each point and an exponentially small gradient.

Appendix D. Detailed analysis on optimizing combination coefficients

The necessary quantum measurements for obtaining the inputs Q, r needed to solve the combination coefficients is discussed in the following lemma. Note that here we are interested in a single sample of each Q_{ij} and r_i, each of which is made up of a sum of terms K_A^2 and K_A, respectively. Hence, each term in the sum is sampled once and the terms are added up to provide the single sample.

Lemma 2 (Measuring the overlap matrix elements). *Given the unitary decomposition of matrix A from assumption 2, the circuit for $|b\rangle$ via assumption 1, and let the circuit for creating $|u_i\rangle$ be W_i. The condition number of A shall be κ. Assume that controllable unitaries of all involved unitaries can be constructed. Then, we can obtain a single sample of $(V^\dagger V)_{ij} = \langle u_i| A^\dagger A |u_j\rangle$ and $q_i = \langle u_i| A^\dagger |b\rangle$ from $O(K_A^2)$ and $\mathcal{O}(K_A)$ quantum measurements, where the magnitude of each sample is bounded by $\mathcal{O}\left(\left(\sum_{i=1}^{K_A}|\beta_k|\right)^2\right) \equiv \mathcal{O}\left(B^2\right)$ and $\mathcal{O}\left(\sum_{i=1}^{K_A}|\beta_k|\right) \equiv \mathcal{O}(B)$, respectively.*

Proof. Note that $\langle u_i| A^\dagger A |u_j\rangle = \sum_{k,k'=1}^{K_A}\beta_k\beta_{k'} \langle 0^n| W_i^\dagger U_k^\dagger U_{k'} W_j |0^n\rangle$. Construct the unitaries $U_{\text{prep},k,k'} = |0\rangle\langle 0| \otimes \mathbb{1} + |1\rangle\langle 1| \otimes W_i^\dagger U_k^\dagger U_{k'} W_j$. Use the Hadamard test via proposition 9 to obtain a single sample for each $\langle 0^n| W_i^\dagger U_k^\dagger U_{k'} W_j |0^n\rangle$. The absolute value of each sample is bounded by $\mathcal{O}(1)$ because the sample for the real and imaginary part are both bounded by 1. Doing this sampling for all k, k' uses $\mathcal{O}\left(K_A^2\right)$ quantum measurements. Then we obtain an estimate for $\mathrm{Re}\left\{\langle u_i| A^\dagger A |u_j\rangle\right\}$, where the absolute value is bounded by $\mathcal{O}\left(\left(\sum_{i=1}^{K_A}|\beta_k|\right)^2\right) = \mathcal{O}\left(B^2\right)$. Similar steps and constructing the unitaries $U_{prep,k,b} = |0\rangle\langle 0| \otimes \mathbb{1} + |1\rangle\langle 1| \otimes W_i^\dagger U_k^\dagger U_b$ allow us to obtain an estimate for $\langle w_i| A^\dagger |b\rangle$ with absolute value bounded by $\mathcal{O}\left(\sum_{i=1}^{K_A}|\beta_k|\right) = \mathcal{O}(B)$ using $\mathcal{O}(K_A)$ quantum measurements. □

Because of the statistical nature of quantum measurements, we can only obtain estimates of Q and r and not their exact values. The following proposition summarizes the required number of measurements to achieve a good solution using the approximations $\hat{Q}$ and $\hat{r}$ obtained from quantum measurement. This proposition focuses on real optimization where the variable z is real.

Proposition 12 (Solving the approximate quadratic problem). *Consider a quadratic function $L(z) = z^T Q z - 2r^T z$, where $Q \in \mathbb{R}^{m\times m}$ is positive definite and $z \in \mathbb{R}^m$. Let $z^* = \arg\min_{z\in\mathbb{R}^m} L(z)$. Let $T > 0$ and let $\hat{Q}$ and $\hat{r}$ be estimates of Q and r such that $\left\|\hat{Q} - Q\right\| \leqslant \mathcal{O}\left(\sqrt{m/T}\right)$ and $\|\hat{r} - r\| \leqslant \mathcal{O}\left(\sqrt{m/T}\right)$. The solution $\hat{z}$ of the quadratic optimation $\hat{L}(z) = z^T\hat{Q}z - 2\hat{r}^T z$, satisfies*

$$L(\hat{z}) - L(z^*) \leqslant \epsilon,$$

if $T > Cm\|Q\|\left\|Q^{-1}\right\|^2(1 + \|z^*\|)^2/\epsilon$, with a constant $C > 0$.

Proof. Let $z^* = Q^{-1}r$ be the solution to the original problem. The solution $\hat{z} = \hat{Q}^{-1}\hat{r}$ minimizes $\hat{L}(z) = z^T\hat{Q}z - 2\hat{r}^T z$. Thus we have $\hat{Q}\hat{z} - Q\hat{z} + Q\hat{z} - Qz^* = \hat{r} - r$. This gives $(\hat{z} - z^*) = Q^{-1}(\hat{r} - r - (\hat{Q} - Q)\hat{z})$. Hence $\|\hat{z} - z^*\| \leqslant \left\|Q^{-1}\right\|(\|\hat{r} - r\| + \left\|\hat{Q} - Q\right\|\|\hat{z}\|) \leqslant \left\|Q^{-1}\right\|\|\hat{r} - r\| + \left\|Q^{-1}\right\|\left\|\hat{Q} - Q\right\|\|z^*\| + \left\|Q^{-1}\right\|\left\|\hat{Q} - Q\right\|\|\hat{z} - z^*\|$. This gives

$$\|\hat{z} - z^*\| \leqslant \frac{\left\|Q^{-1}\right\|(\|\hat{r} - r\| + \left\|\hat{Q} - Q\right\|\|z^*\|)}{1 - \left\|Q^{-1}\right\|\left\|\hat{Q} - Q\right\|} \leqslant \sqrt{\epsilon/\|Q\|}.$$

The last inequality requires setting $T > Cm\|Q\|\left\|Q^{-1}\right\|^2(1+\|z^*\|)^2/\epsilon$, with a constant C, such that $1-\left\|Q^{-1}\right\|\left\|\hat{Q}-Q\right\| \geqslant 1/2$ and $\left\|Q^{-1}\right\|(\|\hat{r}-r\|+\left\|\hat{Q}-Q\right\|\|z^*\|) \leqslant \frac{1}{2}\sqrt{\epsilon/\|Q\|}$. Because $L(z)$ has zero gradient at z^*, we have

$$L(\hat{z})-L(z^*) \leqslant \|Q\|\,\|\hat{z}-z^*\|^2 \leqslant \epsilon.$$

□

The following is a detailed statement on the hardness of optimizing combination coefficients.

Proposition 13. *For any Hermitian matrix $A \in \mathbb{C}^{2^n\times 2^n}$ satisfying assumption 2, any $\mathcal{O}\left(\mathrm{poly}(n)\right)$ quantum circuit generating $|b\rangle \in \mathbb{C}^{2^n}$, and any two $\mathcal{O}\left(\mathrm{poly}(n)\right)$ quantum circuits generating $|u_1\rangle, |u_2\rangle \in \mathbb{C}^{2^n\times 2^n}$, assume there exists a classical algorithm to output $\hat{\alpha}_1, \hat{\alpha}_2 \in \mathbb{C}$, such that*

$$L_{\mathrm{Reg}}\left(\sum_{i=1}^{2}\hat{\alpha}_i|u_i\rangle\right) \leqslant \min_{\alpha_1,\alpha_2\in\mathbb{C}} L_{\mathrm{Reg}}\left(\sum_{i=1}^{2}\alpha_i|u_i\rangle\right)+\epsilon, \tag{D1}$$

in time $\mathcal{O}\left(\mathrm{poly}(n)\right)$. Then BQP = BPP.

Proof. Given a problem in BQP, any quantum algorithm to solve it can be expressed as a quantum circuit consisting of T single- and two-qubit gates $U_1,\ldots,U_T$ acting on n qubits, where n is polynomially related to the input size of the problem and includes ancillas, and $T=\mathcal{O}\left(\mathrm{poly}(n)\right)$. The problem can be solved up to small error by determining the probability of measuring 0 in the first qubit after applying $U_1,\ldots,U_T$ on $|0^n\rangle$, $P_0 \equiv \langle 0^n|U_1^\dagger\ldots U_T^\dagger(|0\rangle\langle 0|\otimes\mathbb{1}\otimes\cdots\otimes\mathbb{1})U_T\ldots U_1|0^n\rangle$. The same is true for the probability of measuring 1, $P_1 = \langle 0^n|U_1^\dagger\ldots U_T^\dagger(|1\rangle\langle 1|\otimes\mathbb{1}\otimes\cdots\otimes\mathbb{1})U_T\ldots U_1|0^n\rangle$. We now construct a linear system of dimension 2^{n+1}, involving $1+n$ qubits where in the notation the first qubit is the newly added one. Let the matrix A be a simple controlled-NOT gate, controlled by the second qubit and acting on the first qubit. Note that A is both Hermitian and unitary, and each entry can be efficiently computed classically. Define three quantum states by

$$|b\rangle = |0\rangle\otimes U_T\ldots U_1|0^n\rangle, \qquad |u_1\rangle = |0\rangle\otimes U_T\ldots U_1|0^n\rangle, \qquad |u_2\rangle = |1\rangle\otimes U_T\ldots U_1|0^n\rangle.$$

We can easily see that $\langle b|A|u_1\rangle = P_0$. Similarly, $\langle b|A|u_2\rangle = P_1$. By assumption there shall be a classical algorithm that can efficiently find $\hat{\alpha}_1,\hat{\alpha}_2\in\mathbb{C}$ that satisfy equation (D1). We now show that $\hat{\alpha}_1,\hat{\alpha}_2$ can be used to infer P_0, P_1. By expansion, we have

$$\left\|A\left(\sum_{i=1}^{2}\alpha_i|u_i\rangle\right)-|b\rangle\right\|_2^2 = |\alpha_1|^2+|\alpha_2|^2-2\,\mathrm{Re}\left\{\alpha_1\langle b|A|u_1\rangle+\alpha_2\langle b|A|u_2\rangle\right\}+1.$$

Using $\langle b|A|u_1\rangle = P_0$ and $\langle b|A|u_2\rangle = P_1$, we have $\left\|A\sum_{i=1}^{2}\alpha_i|u_i\rangle-|b\rangle\right\|_2^2 = |\alpha_1-P_0|^2+|\alpha_2-P_1|^2+(1-P_0^2-P_1^2)$. The optimal combination parameters are $\alpha_1=P_0$ and $\alpha_2=P_1$. Hence equation (D1) can be rewritten as

$$|\hat{\alpha}_1-P_0|^2+|\hat{\alpha}_2-P_1|^2+(1-P_0^2-P_1^2) \leqslant (1-P_0^2-P_1^2)+\epsilon \implies |\hat{\alpha}_1-P_0|^2+|\hat{\alpha}_2-P_1|^2 \leqslant \epsilon.$$

This means the algorithm can use $\hat{\alpha}_1,\hat{\alpha}_2$ to determine P_0 and P_1, which solves the BQP problem. □

Appendix E. Provable guarantee for the ansatz tree approach

We provide proof for the propositions of the main text. Proposition 4 is a simple extension and variation of known results on using polynomial approximation of $1/x$ to solve linear systems of equations [47].

Proof of proposition 4. By including all nodes $\{|u_1\rangle,\ldots,|u_m\rangle\}$ on the ansatz tree with depth at most $O(\kappa\log(\kappa/\epsilon))$, the subspace contains $p(A)|b\rangle$ for any polynomial $p(\cdot)$ with degree at most $O(\kappa\log(\kappa/\epsilon))$. In lemma 14 in [47], it was shown that there exists a set of constants $p_j, \forall j=0,\ldots,j_0$ such that $p(z)=\sum_{j=0}^{j_0}p_jz^j$ is ϵ-close to z^{-1} in the domain $D_\kappa=[-1,-1/\kappa]\cup[1/\kappa,1]\cup\{0\}$, where $j_0 = 2\sqrt{\kappa^2\log(2\kappa/\epsilon)\log(8\kappa^2\log(2\kappa/\epsilon)/\epsilon)}+1 = O(\kappa\log(\kappa/\epsilon))$. Using the condition that $\|A\|=1$ and $\left\|A^{-1}\right\|=\kappa$, we know that all the eigenvalues of A lie in the domain D_κ. Because $p(z)$ is ϵ-close to z^{-1} in the domain D_κ, we thus have $\left\|p(A)-A^{-1}\right\|\leqslant\epsilon$. This implies that $\left\|p(A)|b\rangle-A^{-1}|b\rangle\right\| \leqslant \left\|p(A)-A^{-1}\right\|\leqslant\epsilon$.

Hence there exists a set of combination parameters $\hat{\alpha}_1, \ldots, \hat{\alpha}_m \in \mathbb{R}$ set according to the coefficients p_j in the polynomial $p(x)$, such that $\hat{x} = \sum_i \hat{\alpha}_i |u_i\rangle$ satisfies $\left\|\hat{x} - A^{-1}|b\rangle\right\|_2 \leqslant \epsilon$. So

$$\min_{\alpha_1,\ldots,\alpha_m \in \mathbb{R}} \left\| A\left(\sum_i \alpha_i |u_i\rangle\right) - |b\rangle \right\|_2^2 \leqslant \|A\hat{x} - |b\rangle\|_2^2 \tag{E1}$$

$$\leqslant \|A\|^2 \left\|\hat{x} - A^{-1}|b\rangle\right\|_2^2 \leqslant \epsilon^2 = \min_{x \in \mathbb{C}^{2^n}} \|Ax - |b\rangle\|_2^2 + \epsilon^2. \tag{E2}$$

The last equality uses the fact that $x = A^{-1}|b\rangle$ satisfy $\|Ax - |b\rangle\|_2 = 0$. Note that we actually achieve ϵ^2 error, which is better than ϵ since $\epsilon < 1$. □

Proof of proposition 5. We first diagonalize A to be $VDV^\dagger$, where D is diagonal and V is a unitary matrix. We also set $N = 2^n$ to be the system size. The eigenvalues of A are denoted as $\lambda_i, \forall i = 1, \ldots, N$. We set $\tilde{b} = V^\dagger |b\rangle$ and note that $\sum_{i=1}^N |\tilde{b}_i|^2 = 1$, as $|b\rangle$ is normalized. We consider a rotated x, $\tilde{x} = V^\dagger x \in \mathbb{C}^N$. Using $\tilde{x}$, the loss function $\frac{1}{2}\|x\|_2^2 + \|Ax - |b\rangle\|_2^2$ can be written as

$$\sum_{i=1}^N \left(\frac{1}{2}|\tilde{x}_i|^2 + |\lambda_i \tilde{x}_i - \tilde{b}_i|^2\right).$$

We can minimize this expression analytically as

$$\tilde{x}_i = \frac{2\lambda_i \tilde{b}_i}{2\lambda_i^2 + 1} \in \mathbb{C}, \quad \forall\, i = 1, \ldots, N.$$

Plugging this optimal solution into the loss function yields

$$\sum_{i=1}^N |\tilde{b}_i|^2 \left(\frac{1}{2}y_i^2 + (\lambda_i y_i - 1)^2\right),$$

where $y_i = 2\lambda_i/(2\lambda_i^2 + 1) \in \mathbb{R}$. We now consider the space of all linear combinations of $A^k|b\rangle$, $\forall\, k = 0, \ldots, K_0$, which is a subspace of $\mathrm{span}(u_1, \ldots, u_m)$. This space is written as $\left\{\sum_{k=0}^{K_0} p_k A^k |b\rangle\right\}$. In this subspace, the loss function can be written as

$$\frac{1}{2}\left\|\sum_k p_k D^k \tilde{b}\right\|_2^2 + \left\|\sum_k p_k D^{k+1}\tilde{b} - \tilde{b}\right\|_2^2 = \sum_{i=1}^N |\tilde{b}_i|^2 \left(\frac{1}{2}\left(\sum_k p_k \lambda_i^k\right)^2 + \left(\lambda_i \sum_k p_k \lambda_i^k - 1\right)^2\right).$$

We now analyze how accurate a polynomial $\sum_k p_k x^k$ can approximate $2x/(2x^2+1)$ within $[-1, 1]$. Due to the condition that $\|A\| \leqslant 1$, we only care about the range $[-1, 1]$. The approximation can be done by performing Chebyshev decomposition of the function $x/(x^2 + 1/2)$,

$$\frac{x}{x^2 + 1/2} = \sum_{k=0,1,2,\ldots} c_k T_{2k+1}(x),$$

where $T_{2k+1}(x)$ is $(2k+1)$th Chebyshev polynomial of the first kind (which is of degree $2k+1$). And we have the following recursive formula for $c_k, \forall k = 0, 1, 2, \ldots,$

$$c_k = (-2 + \sqrt{3})^k \left(1 - \frac{1}{\sqrt{3}}\right).$$

If we truncate the Chebyshev expansion at $\lfloor (K_0 - 1)/2 \rfloor$ (the degree is at most K_0), then

$$\sup_{x \in [-1,1]} \left| \frac{x}{x^2 + 1/2} - \sum_{k=0}^{\lfloor (K_0-1)/2 \rfloor} c_k T_{2k+1}(x) \right| \leqslant \sum_{\lfloor (K_0-1)/2 \rfloor + 1}^{\infty} |c_k| \leqslant \frac{(2-\sqrt{3})^{K_0/2}\left(1 - \frac{1}{\sqrt{3}}\right)}{\sqrt{3} - 1} \equiv \xi.$$

By choosing p_k according to c_k and the Chebyshev polynomial coefficients, we have

$$\left| y_i - \sum_{k=0}^{K_0} p_k \lambda_i^k \right| \leqslant \xi, \quad \forall\, i = 1, \ldots, N.$$

Then using $\frac{1}{2}z^2 + (\lambda_i z - 1)^2 = \frac{1}{2}y_i^2 + (\lambda_i y_i - 1)^2 + (\frac{1}{2} + \lambda_i^2)(z - y_i)^2,\ \forall\, z \in \mathbb{R}$, we have

$$\frac{1}{2}\left(\sum_k p_k \lambda_i^k\right)^2 + \left(\lambda_i \sum_k p_k \lambda_i^k - 1\right)^2 \leqslant \frac{1}{2}y_i^2 + (\lambda_i y_i - 1)^2 + \left(\frac{1}{2} + \lambda_i^2\right)\xi^2, \quad \forall\, i = 1, \ldots, N.$$

Using the fact that $|\lambda_i| \leqslant 1$ and $\sum_i |\tilde{b}_i|^2 = 1$, we have

$$\sum_{i=1}^N |\tilde{b}_i|^2 \left(\frac{1}{2}\left(\sum_k p_k \lambda_i^k\right)^2 + \left(\lambda_i \sum_k p_k \lambda_i^k - 1\right)^2\right) \leqslant \min_{x \in \mathbb{C}^{2^n}} \left(\frac{1}{2}\|x\|_2^2 + \|Ax - |b\rangle\|_2^2\right) + \frac{3}{2}\xi^2.$$

Now we want $\frac{3}{2}\xi^2 \leqslant \epsilon$ by choosing a large enough K_0. Using $\xi = \frac{(2-\sqrt{3})^{K_0/2}}{\sqrt{3}}$, we need $(2 - \sqrt{3})^{K_0} \leqslant 2\epsilon$. By choosing $K_0 \geqslant \log(1/2\epsilon)/\log(1/(2 - \sqrt{3}))$, we are guaranteed to have

$$\min_{\alpha_1, \ldots, \alpha_m \in \mathbb{R}} \left(\frac{1}{2}\left\|\sum_i \alpha_i u_i\right\|_2^2 + \left\|A\left(\sum_i \alpha_i u_i\right) - |b\rangle\right\|_2^2\right) \leqslant \min_{x \in \mathbb{C}^{2^n}} \left(\frac{1}{2}\|x\|_2^2 + \|Ax - |b\rangle\|_2^2\right) + \epsilon.$$

□

Proof of proposition 7. Consider the loss function on $x^S + \alpha\,|u^*\rangle$, where $\alpha \in \mathbb{C}$. Because x^S is a linear combination of $|u_i\rangle \in S$ and $L_{\text{Reg}}(x) = \|Ax - b\|_2^2$, we know that the optimal combination of $S \cup \{|u^*\rangle\}$ satisfies

$$\min_{\alpha_1, \ldots, \alpha_{m+1} \in \mathbb{C}} L_{\text{Reg}}\left(\sum_{|u_i\rangle \in S \cup \{|u^*\rangle\}} \alpha_i\,|u_i\rangle\right) \leqslant L_{\text{Reg}}(x^S + \alpha\,|u^*\rangle),$$

for any $\alpha \in \mathbb{C}$. By expanding $L_{\text{Reg}}(x^S + \alpha\,|u^*\rangle)$, we have ($\overline{\alpha}$ denotes the complex conjugated α)

$$L_{\text{Reg}}(x^S + \alpha\,|u^*\rangle) = L_{\text{Reg}}(x^S) + |\alpha|^2 \langle u^*|\, A^\dagger A\,|u^*\rangle + \text{Re}\left\{\overline{\alpha}\,\langle u^*|\, \nabla L_{\text{Reg}}(x^S)\right\}.$$

By selecting $\alpha = -\overline{\langle u^*|\, \nabla L_{\text{Reg}}(x^S)}/2\,\langle u^*|\, A^\dagger A\,|u^*\rangle$, we have

$$L_{\text{Reg}}(x^S + \alpha\,|u^*\rangle) = L_{\text{Reg}}(x^S) - \frac{|\langle u^*|\, \nabla L_{\text{Reg}}(x^S)|^2}{4\,\langle u^*|\, A^\dagger A\,|u^*\rangle} \leqslant \min_{\alpha_1, \ldots, \alpha_m \in \mathbb{C}} L_{\text{Reg}}\left(\sum_{|u_i\rangle \in S} \alpha_i\,|u_i\rangle\right) - \frac{g^2}{4}.$$

The last inequality uses the assumption that the spectral radius of A is no greater than 1. □

Appendix F. Experiments on solving linear systems using agnostic ansätze

We discuss our experiments on solving linear systems using the agnostic ansatz in detail. We focus on solving the real-valued version of equation (1). By construction, our agnostic ansatz is constrained to explore the solution vector in the real subspace of the appropriate Hilbert space. The two real gates we use are the single-qubit rotation around the y-axis for every qubit with tunable angle (the variational parameter) and the CNOT gate. Thus, a single layer of our n-qubit variational circuit consists of n variational parameters and a certain pattern of CNOT gates. We implement various types of agnostic ansätze depending on how the CNOT gates are applied. The topology of a quantum computer favours a particular arrangement of CNOT gates over another and our exploration for different ansätze is motivated by the same. Here, we enumerate the different variational ansätze. We label our qubits from 1 to n and denote the same by $[1, \ldots, n]$. The CNOT gate between qubit i (control) and j (target) will be denoted by $C(i, j)$.

(a) Star ansatz: the qubit numbered 1 is always the control, while target ranges over all $i \in [2, \ldots, n]$. In other words, we apply $C(1, i)$ for all $i \in [2, \ldots, n]$.

(b) Line ansatz: the ansatz contains $C(i, i + 1)$ for every $i \in [1, \ldots, n - 1]$.

(c) Ring ansatz: It is similar to the line ansatz with the difference that there is an extra CNOT gate at the boundary, i.e. $C(n, 1)$.

(d) Complete graph ansatz: we implement $C(i, j)$ for every $i, j \in [1, \ldots, n]$ such that $i \neq j$.

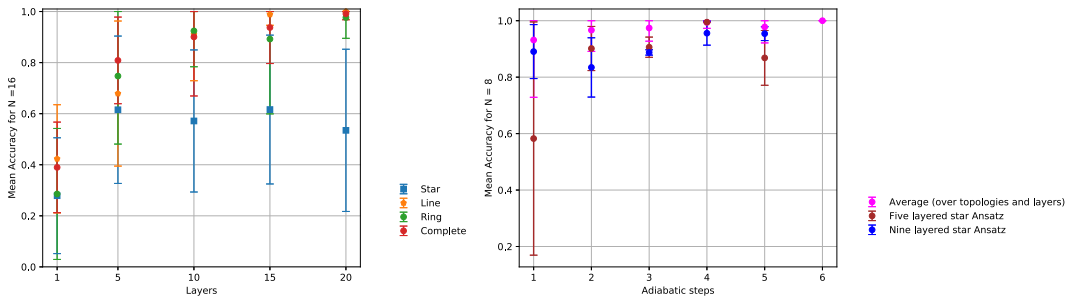

Figure 5. Numerical experiments on solving linear systems using agnostic ansätze. Left: the mean accuracy versus circuit layer depth for various ansätze employed to solve linear systems for $N = 16$ is shown. The mean accuracy goes to unity for line graph, ring graph and complete graph ansätze with a 20-layer circuit. The star-graph ansatz performs performs worst and eventually levels at accuracy 0.6. Right: we implement the AAVQE approach for $N = 8$ and see improvement over standard VQE (adiabatic steps $= 1$) over an average of all ansätze and number of layers. Employing more adiabatic steps also improves the mean accuracy. For example, the mean accuracy for the five and nine layered star ansätze improves to 1.0 as we increase the number of adiabatic steps from 1 to 6. The dots represent the mean accuracy and the bars represent the spread corresponding to a standard deviation with the upper and lower cutoffs as 1 and 0 respectively.

We note that these ansätze may not be computationally universal and only form a subset of all possible quantum circuits. We note discussions on the computational universality of QAOA in references [62, 63].

We have conducted numerical experiments on Rigetti quantum virtual machine where the linear systems are generated randomly over different system sizes ($N = 2, 4, 8, 16$). Some of the numerical results can be seen in figure 5. The figure of merit is mean accuracy, which is the average fidelity of the output vector and the solution over 100 independent runs. In figure 5 (left), we present the use of standard VQE for solving linear systems with $N = 16$. We can see a rise in overall performance as we increase the number of layers. The mean accuracy goes to unity for most CNOT gate patterns except for the star graph. The performance for the star graph starts improving but soon levels at mean accuracy of 0.6.

In figure 5 (right), we show the AAVQE approach for $N = 8$. The purple/magenta data points are an average over all the topologies and different layers. We can see an improvement by roughly 10% using AAVQE (adiabatic steps $= 6$) over standard VQE (adiabatic steps $= 1$). We can also see that as we increase the number of adiabatic steps, the performance of AAVQE becomes better. The mean accuracy for all settings considered here becomes very close to unity as we increase the number of adiabatic steps to 6. Furthermore, the standard deviation around the mean accuracy goes below 10^{-2}. As such, most of the settings were able to achieve the accuracy of close to 1.0 in AAVQE, which is not achieved with standard VQE (adiabatic steps $= 1$).

References

[1] Harrow A W, Hassidim A and Lloyd S 2009 *Phys. Rev. Lett.* **103** 150502
[2] van Apeldoorn J, Gilyén A, Gribling S and de Wolf R 2018 arXiv:1809.00643
[3] Chakrabarti S, Childs A M, Li T and Wu X 2018 arXiv:1809.01731
[4] van Apeldoorn J and Gilyén A 2017 *Proc. of the 46th Int. Coll. on Automata, Languages, and Programming, ICALP'19*
[5] Li T, Chakrabarti S and Wu X 2019 arXiv:1904.02276
[6] Brandão F G S L, Kalev A, Li T, Lin C Y, Svore K M and Wu X 2019 *46th Int. Coll. on Automata, Languages, and Programming, ICALP 2019* (Patras, Greece 9th July –12th July 2019) pp 27:1–27:14
[7] Preskill J 2018 *Quantum* **2** 79
[8] Preskill J 2012 arXiv:1203.5813
[9] Aaronson S and Chen L 2016 arXiv:1612.05903
[10] Harrow A W and Montanaro A 2017 *Nature* **549** 203
[11] Neill C *et al* 2018 *Science* **360** 195
[12] Arute F *et al* 2019 *Nature* **574** 505
[13] Zhong H-S *et al* 2020 *Science* **370** 1460
[14] Aaronson S and Arkhipov A 2011 *Proc. of the Forty-Third Annual ACM Symp. on Theory of Computing* (New York: ACM) pp 333–42
[15] Bouland A, Fefferman B, Nirkhe C and Vazirani U 2019 *Nat. Phys.* **15** 159
[16] Bharti K *et al* 2021 arXiv:2101.08448
[17] Cerezo M *et al* 2020 arXiv:2012.09265
[18] Peruzzo A, McClean J, Shadbolt P, Yung M-H, Zhou X-Q, Love P J, Aspuru-Guzik A and O'Brien J L 2014 *Nat. Commun.* **5** 4213
[19] McClean J R, Romero J, Babbush R and Aspuru-Guzik A 2016 *New J. Phys.* **18** 023023
[20] Kandala A, Mezzacapo A, Temme K, Takita M, Brink M, Chow J M and Gambetta J M 2017 *Nature* **549** 242
[21] Farhi E, Goldstone J and Gutmann S 2014 arXiv:1411.4028
[22] Farhi E and Harrow A W 2016 arXiv:1602.07674
[23] Childs A M, Kothari R and Somma R D 2015 arXiv:1511.02306
[24] Berry D W, Childs A M, Cleve R, Kothari R and Somma R D 2015 *Phys. Rev. Lett.* **114** 090502

[25] Gilyén A, Su Y, Low G H and Wiebe N 2019 *Proc. of the 51st Annual ACM SIGACT Symp. on Theory of Computing, STOC 2019* (New York: Association for Computing Machinery) pp 193–204
[26] Low G H and Chuang I L 2017 *Phys. Rev. Lett.* **118** 010501
[27] Low G H and Chuang I L 2019 *Quantum* **3** 163
[28] An D and Lin L 2019 arXiv:1909.05500
[29] Subaşı Y, Somma R D and Orsucci D 2019 *Phys. Rev. Lett.* **122** 060504
[30] Bravo-Prieto C, LaRose R, Cerezo M, Subasi Y, Cincio L and Coles P J 2019 arXiv:1909.05820
[31] Lagarias J C, Reeds J A, Wright M H and Wright P E 1998 *SIAM J. Optim.* **9** 112
[32] Li Y and Benjamin S C 2017 *Phys. Rev.* X **7** 021050
[33] McArdle S, Jones T, Endo S, Li Y, Benjamin S C and Yuan X 2019 *npj Quantum Information* **5** 1
[34] Farhi E, Goldstone J, Gutmann S and Sipser M 2000 arXiv:quant-ph/0001106
[35] Lloyd S 1996 *Science* **273** 1073
[36] Berry D W, Childs A M and Kothari R 2015 *2015 IEEE 56th Annual Symp. on Foundations of Computer Science* (Piscataway, NJ: IEEE) pp 792–809
[37] Xu X, Sun J, Endo S, Li Y, Benjamin S C and Yuan X 2019 arXiv:1909.03898
[38] McClean J R, Boixo S, Smelyanskiy V N, Babbush R and Neven H 2018 *Nat. Commun.* **9** 4812
[39] Ng A Y 2004 *Proc. of the Twenty-First Int. Conf. on Machine Learning* (New York: ACM) p 78
[40] Hoerl A E and Kennard R W 1970 *Technometrics* **12** 55
[41] McArdle S, Jones T, Endo S, Li Y, Benjamin S and Yuan X 2018 arXiv:1804.03023
[42] Wecker D, Hastings M B and Troyer M 2015 *Phys. Rev.* A **92** 042303
[43] Garcia-Saez A and Latorre J 2018 arXiv:1806.02287
[44] Smith R S, Curtis M J and Zeng W J 2016 A practical quantum instruction set architecture arXiv:1608.03355
[45] Hadfield S, Wang Z, O'Gorman B, Rieffel E G, Venturelli D and Biswas R 2019 *Algorithms* **12** 34
[46] Bandeira A S *et al* 2016 *Ann. Probab.* **44** 2479
[47] Childs A M, Kothari R and Somma R D 2017 *SIAM J. Comput.* **46** 1920
[48] Nocedal J and Wright S 2006 *Numerical Optimization* (Berlin: Springer)
[49] Boyd S and Vandenberghe L 2004 *Convex Optimization* (Cambridge: Cambridge University Press)
[50] Chia N-H, Gilyén A, Li T, Lin H-H, Tang E and Wang C 2019 arXiv:1910.06151
[51] O'Malley P J *et al* 2016 *Phys. Rev.* X **6** 031007
[52] Colless J I, Ramasesh V V, Dahlen D, Blok M S, Kimchi-Schwartz M, McClean J, Carter J, De Jong W and Siddiqi I 2018 *Phys. Rev.* X **8** 011021
[53] Moll N *et al* 2018 *Quantum Sci. Technol.* **3** 030503
[54] Wang Z, Hadfield S, Jiang Z and Rieffel E G 2018 *Phys. Rev.* A **97** 022304
[55] Čížek J 1966 *J. Chem. Phys.* **45** 4256
[56] Monkhorst H J 1977 *Int. J. Quantum Chem.* **12** 421
[57] Purvis G D III and Bartlett R J 1982 *J. Chem. Phys.* **76** 1910
[58] Bartlett R J 1989 *J. Phys. Chem.* **93** 1697
[59] LaRose R, Tikku A, O'Neel-Judy É, Cincio L and Coles P J 2019 *npj Quantum Information* **5** 8
[60] Khatri S, LaRose R, Poremba A, Cincio L, Sornborger A T and Coles P J 2019 *Quantum* **3** 140
[61] Brandão F G S L, Harrow A W and Horodecki M 2016 *Commun. Math. Phys.* **346** 397
[62] Lloyd S 2018 arXiv:1812.11075
[63] Morales M E S, Biamonte J D and Zimborás Z 2020 *Quant. Inf. Process.* **19** 291